

Some Possibilities with Polarized Targets

D. Keller
UVA



Outline

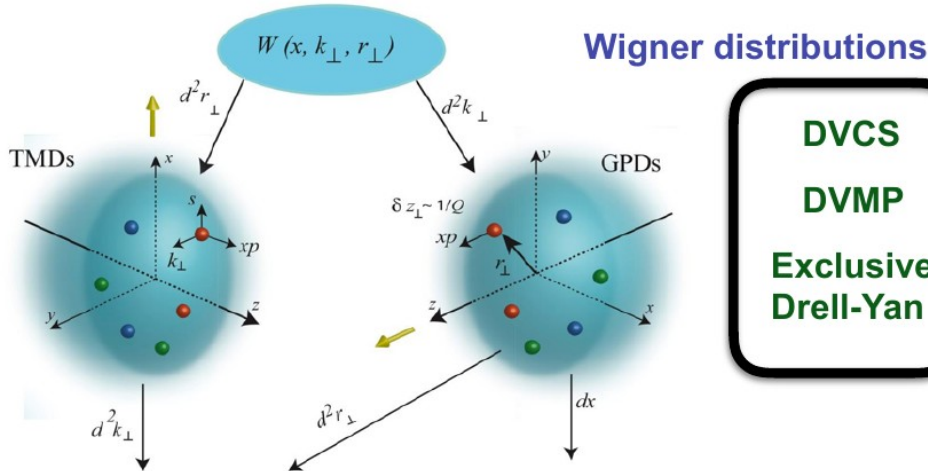
- Understanding Internal Structure
- Introduction to The Target
- Spin-1 Solid Polarized Target
- High Intensity Photon Source
- Conclusion



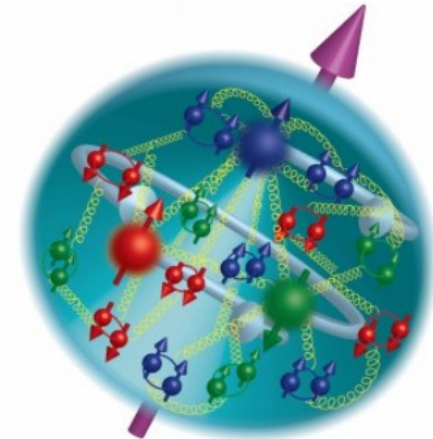
Understanding Dynamics

5D
SIDIS
Drell-Yan

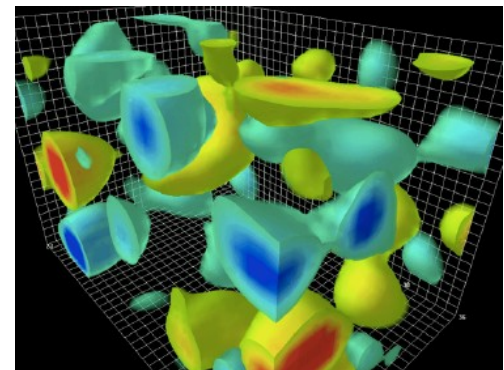
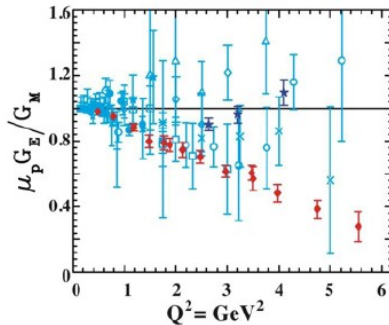
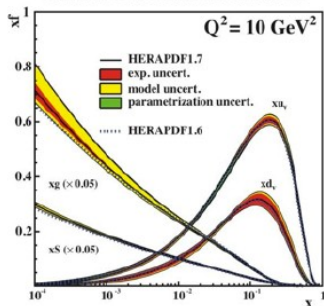
3D



DVCS
DVMP
Exclusive
Drell-Yan

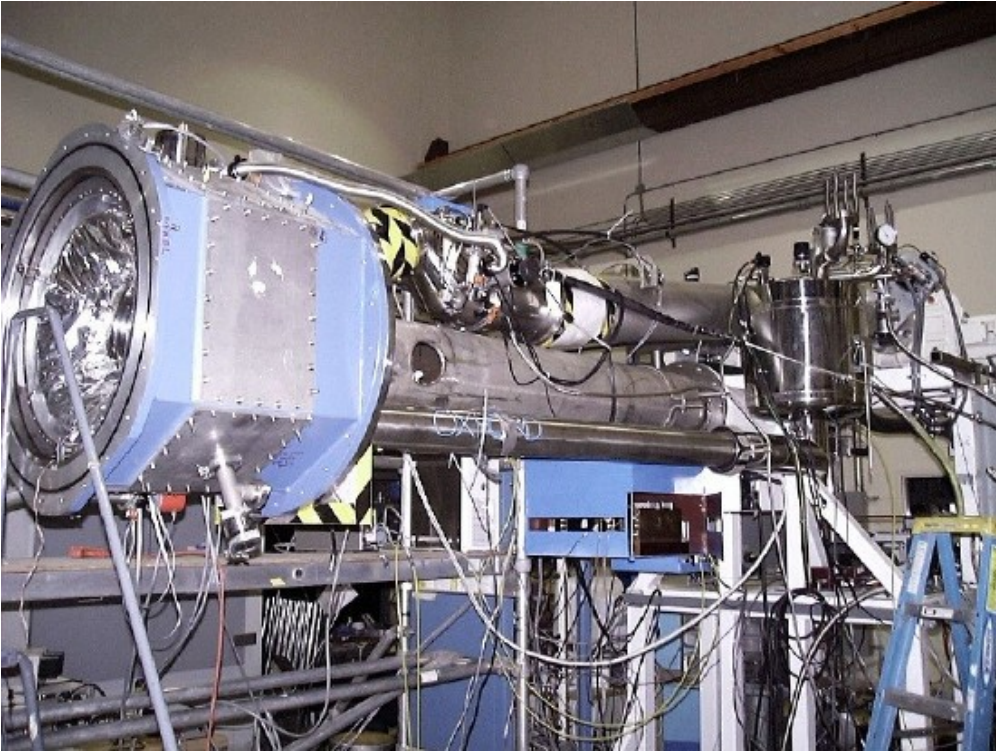


1D



- Need Additional Tools
- Need Complete Framework

What is a Solid Polarized Target

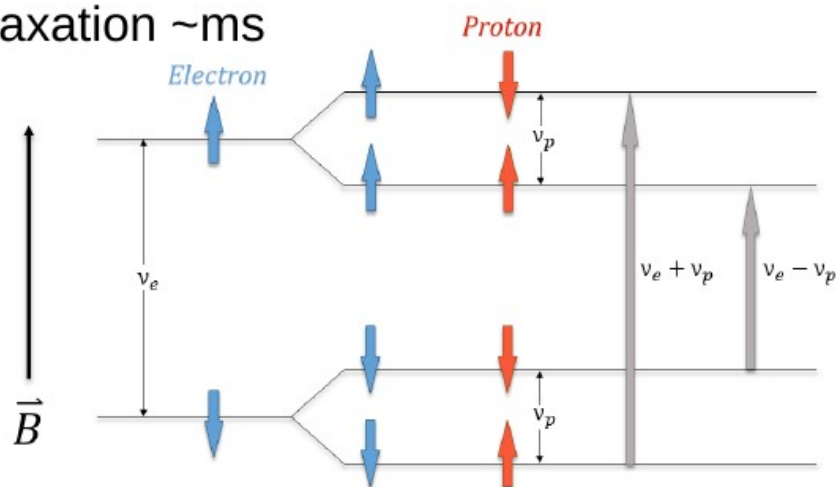


- A marriage of sciences for the purpose of optimizing the over all figure of merit of Nuclear/Particle Spin Physics
- Use of high density, high polarizability, with high interaction rate in fixed target experiments

Dynamic Nuclear Polarization

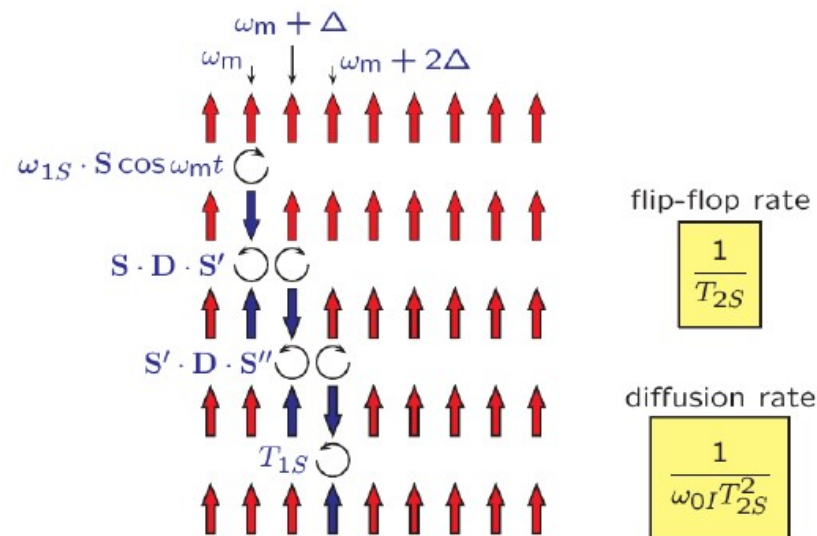
Add Free Radicals, cool sample, RF-sample in B-field

e^- relaxation \sim ms



Zeeman Splitting

5T: 140 GHz
2.5: 70 GHz



narrow ESR line $< \omega_0I$

well-resolved
solid effect

broad ESR line $> \omega_0I$

weak μ -wave field $\omega_1S T_{2S} < 1$

fast spectral diffusion $\frac{1}{\omega_0I T_{2S}^2} > \frac{1}{T_{1S}}$

thermal mixing

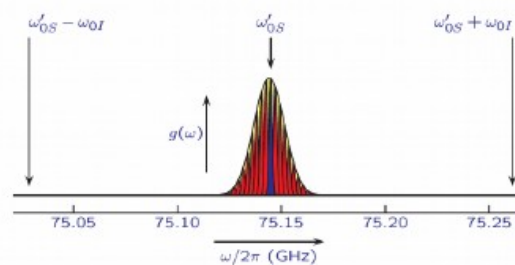
slow spectral diffusion $\frac{1}{\omega_0I T_{2S}^2} < \frac{1}{T_{1S}}$

cross effect

strong μ -field $\omega_1S T_{2S} > 1$

differential
solid effect

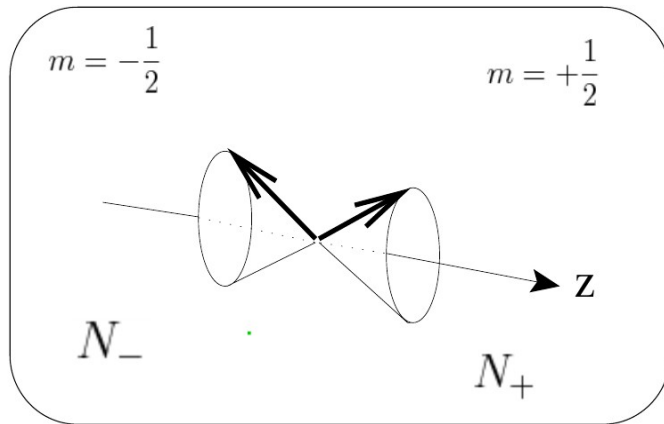
- Transfer of spin polarization from electrons to nuclei
- Electrons 1K 2.5T \sim 92%
- Protons 1K 2.5T \sim 0.25%
- Narrow ESR width will help optimize



$$P = \frac{e^{\frac{\mu B}{kT}} - e^{-\frac{\mu B}{kT}}}{e^{\frac{\mu B}{kT}} + e^{-\frac{\mu B}{kT}}} = \tanh\left(\frac{\mu B}{kT}\right)$$

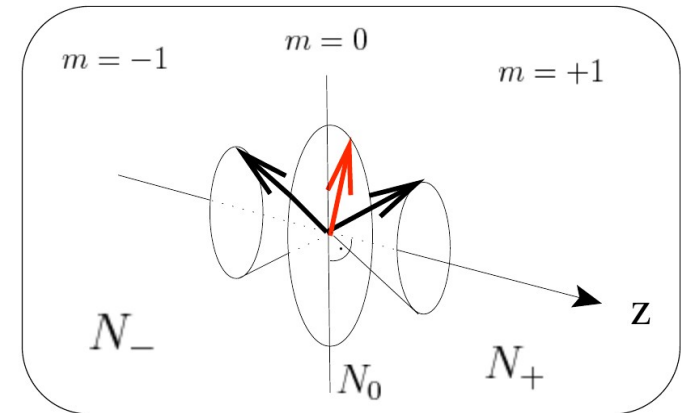
Spin Polarization

Spin-1/2 system in B-field leads to 2 sublevels due to Zeeman interaction



$$P_z = \frac{N_+ - N_-}{N_+ + N_-}$$

$$-1 < P_z < +1$$

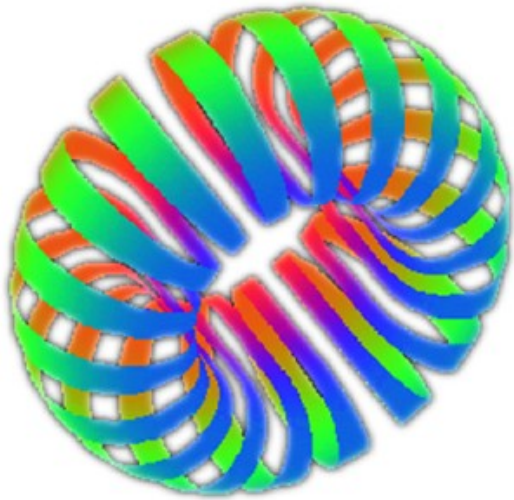


$$P_z = \frac{N_+ - N_-}{N_+ + N_-}$$

$$P_{zz} = \frac{(N_+ - N_0) - (N_0 - N_-)}{N_+ + N_0 + N_-} = \frac{(N_+ + N_-) - 2N_0}{N_+ + N_0 + N_-}$$

Defining Polarization

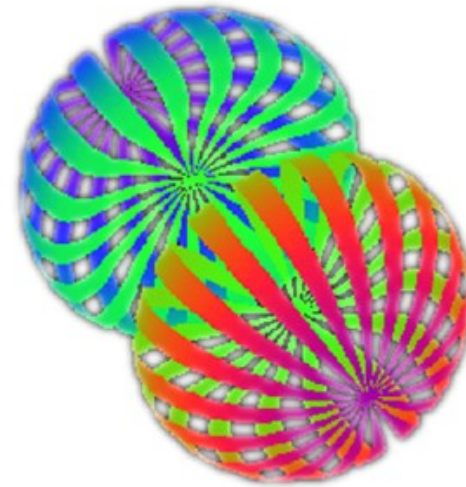
Spin-1



$$P_{zz} = -2$$

Pure Tensor Polarization

All spins in the $m=0$ level

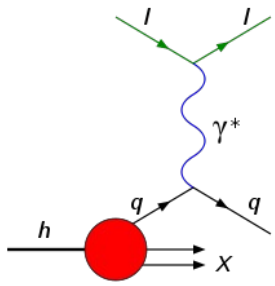


$$P_{zz} = +1$$

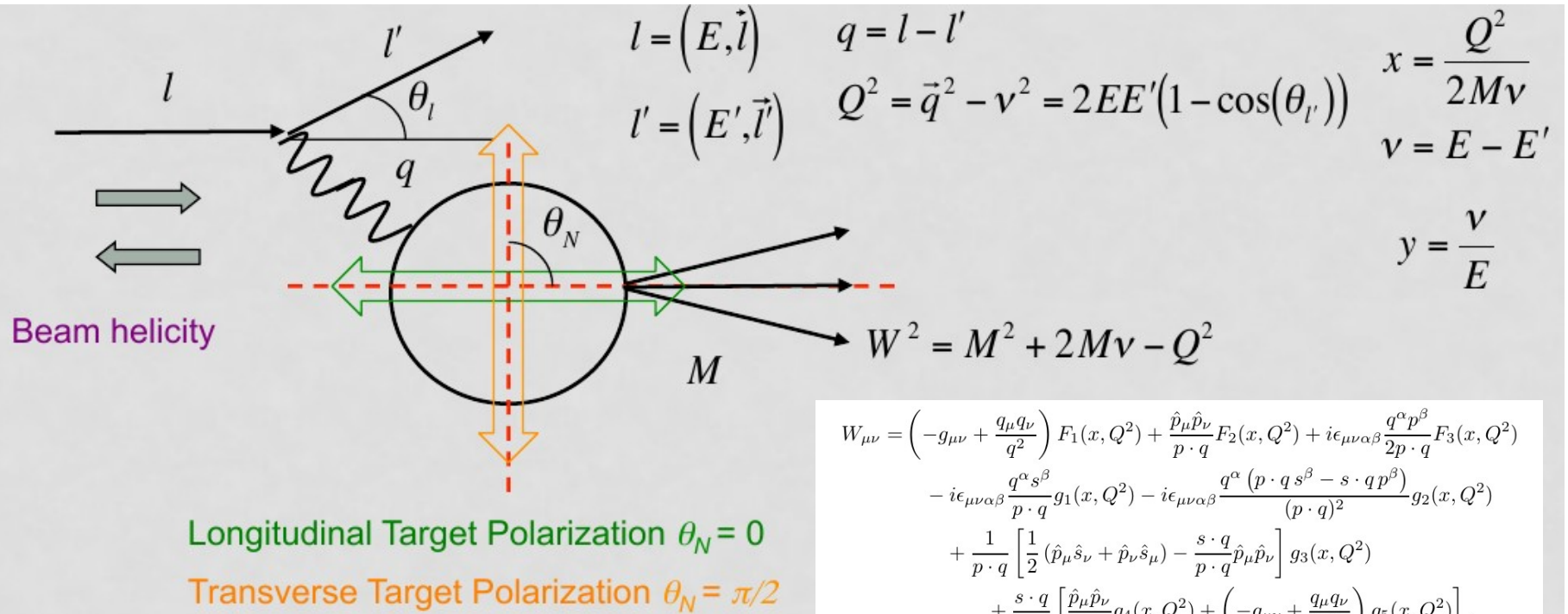
Pure Vector Polarization

$m=0$ level depopulated

$$-2 < P_{zz} < +1$$



Polarized DIS

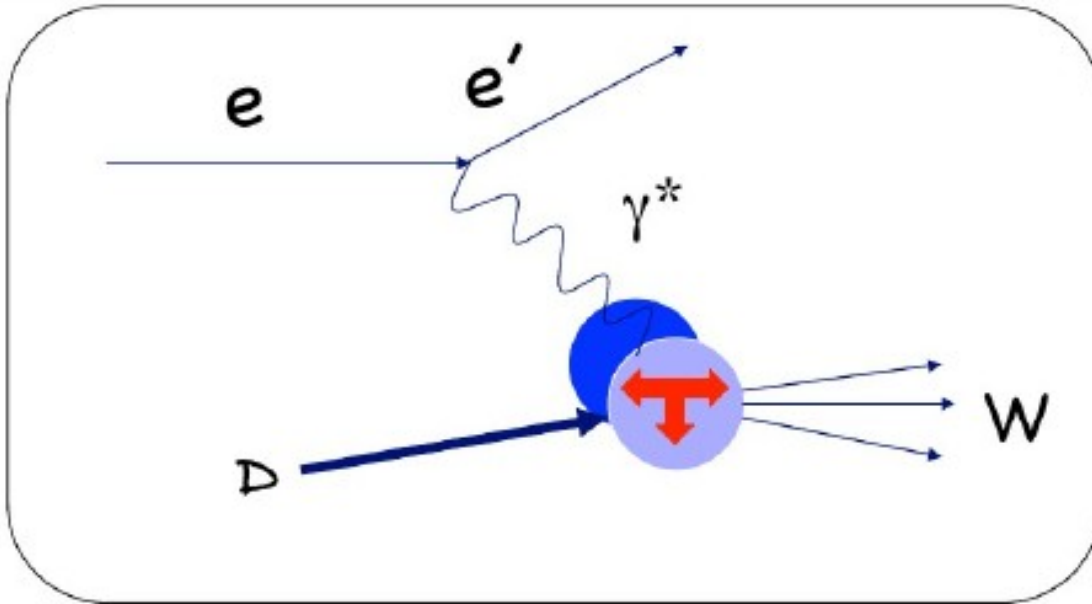


$$\begin{aligned}
 W_{\mu\nu} = & \left(-g_{\mu\nu} + \frac{q_\mu q_\nu}{q^2} \right) F_1(x, Q^2) + \frac{\hat{p}_\mu \hat{p}_\nu}{p \cdot q} F_2(x, Q^2) + i\epsilon_{\mu\nu\alpha\beta} \frac{q^\alpha p^\beta}{2p \cdot q} F_3(x, Q^2) \\
 & - i\epsilon_{\mu\nu\alpha\beta} \frac{q^\alpha s^\beta}{p \cdot q} g_1(x, Q^2) - i\epsilon_{\mu\nu\alpha\beta} \frac{q^\alpha (p \cdot q s^\beta - s \cdot q p^\beta)}{(p \cdot q)^2} g_2(x, Q^2) \\
 & + \frac{1}{p \cdot q} \left[\frac{1}{2} (\hat{p}_\mu \hat{s}_\nu + \hat{p}_\nu \hat{s}_\mu) - \frac{s \cdot q}{p \cdot q} \hat{p}_\mu \hat{p}_\nu \right] g_3(x, Q^2) \\
 & + \frac{s \cdot q}{p \cdot q} \left[\frac{\hat{p}_\mu \hat{p}_\nu}{p \cdot q} g_4(x, Q^2) + \left(-g_{\mu\nu} + \frac{q_\mu q_\nu}{q^2} \right) g_5(x, Q^2) \right],
 \end{aligned}$$

Asymmetries in the scattering of polarized leptons on polarized nucleons most sensitive to spin structure functions g_1 and g_2

$$\frac{d^2\sigma^{\uparrow\uparrow(\downarrow\downarrow)}}{d\Omega dE'} = \frac{d^2\sigma}{d\Omega dE'} - (+) \frac{2\alpha^2 E'}{Q^2 E} \left(\frac{E + E' \cos\theta}{Mv} g_1(x, Q^2) - \frac{Q^2}{Mv^2} g_2(x, Q^2) \right)$$

Novel Targets for Novel Physics



Construct the most general
Tensor W consistent with
Lorentz and gauge invariance

Frankfurt & Strikman (1983)

Hoodbhoy, Jaffe, Manohar (1989)

$$W_{\mu\nu} = -F_1 g_{\mu\nu} + F_2 \frac{P_\mu P_\nu}{\nu}$$

$$+ i \frac{g_1}{\nu} \epsilon_{\mu\nu\lambda\sigma} q^\lambda s^\sigma + i \frac{g_2}{\nu^2} \epsilon_{\mu\nu\lambda\sigma} q^\lambda (p \cdot q s^\sigma - s \cdot q p^\sigma)$$

$$- b_1 r_{\mu\nu} + \frac{1}{6} b_2 (s_{\mu\nu} + t_{\mu\nu} + u_{\mu\nu})$$

$$+ \frac{1}{2} b_3 (s_{\mu\nu} - u_{\mu\nu}) + \frac{1}{2} b_4 (s_{\mu\nu} - t_{\mu\nu})$$

Nucleon

Deuteron

$$F_1 \quad \frac{1}{2} \sum_q e_q^2 [q_\uparrow^{\frac{1}{2}} + q_\uparrow^{-\frac{1}{2}}] \quad \frac{1}{3} \sum_q e_q^2 [q_\uparrow^1 + q_\uparrow^{-1} + q_\uparrow^0]$$

$$g_1 \quad \frac{1}{2} \sum_q e_q^2 [q_\uparrow^{\frac{1}{2}} - q_\uparrow^{-\frac{1}{2}}] \quad \frac{1}{2} \sum_q e_q^2 [q_\uparrow^1 - q_\uparrow^{-1}]$$

$$b_1 \quad -- \quad \frac{1}{2} \sum_q e_q^2 [2q_\uparrow^0 - (q_\uparrow^1 + q_\uparrow^{-1})]$$

} **Tensor Polarization**

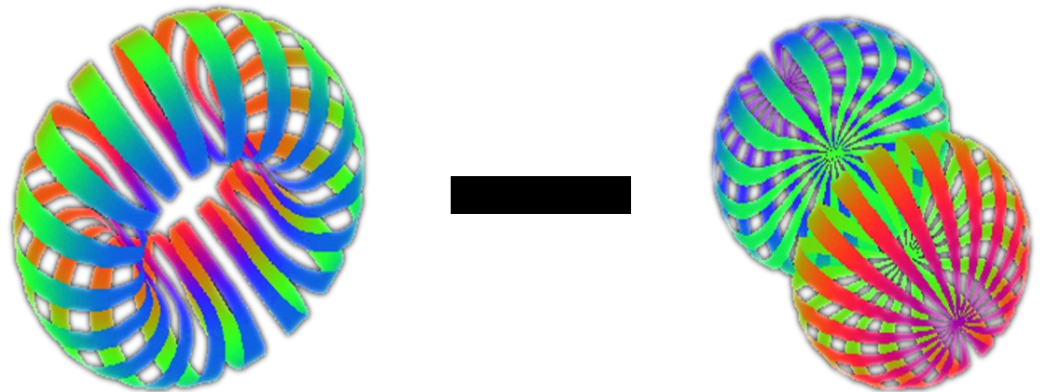
Probing Polarization of Partons

Resulting in the spin structure observed in the nuclear spin

q^0 : Probability to scatter from a quark (any flavor) carrying momentum fraction x while the *Deuteron* is in state $m=0$

q^1 : Probability to scatter from a quark (any flavor) carrying momentum fraction x while the *Deuteron* is in state $|m| = 1$

$$b_1(x) = \frac{q^0(x) - q^1(x)}{2}$$



Tensor-Polarized Structure

Magnetic Moment(D) \approx Magnetic Moment(p)+Magnetic Moment(n)

$$\text{S wave: } \delta_T q_i(x, Q^2) = q_i^0 - \frac{q_i^1 + q_i^{-1}}{2} = 0, \quad b_1 = \frac{1}{2} \sum_i e_{ii}^2 (\delta_T q_i(x, Q^2) + \delta_T \bar{q}_i(x, Q^2)) = 0$$

$$\text{S-D Mix: } \delta_T q_i(x, Q^2) = q_i^0 - \frac{q_i^1 + q_i^{-1}}{2} \neq 0, \quad b_1 = \frac{1}{2} \sum_i e_{ii}^2 (\delta_T q_i(x, Q^2) + \delta_T \bar{q}_i(x, Q^2)) \neq 0$$

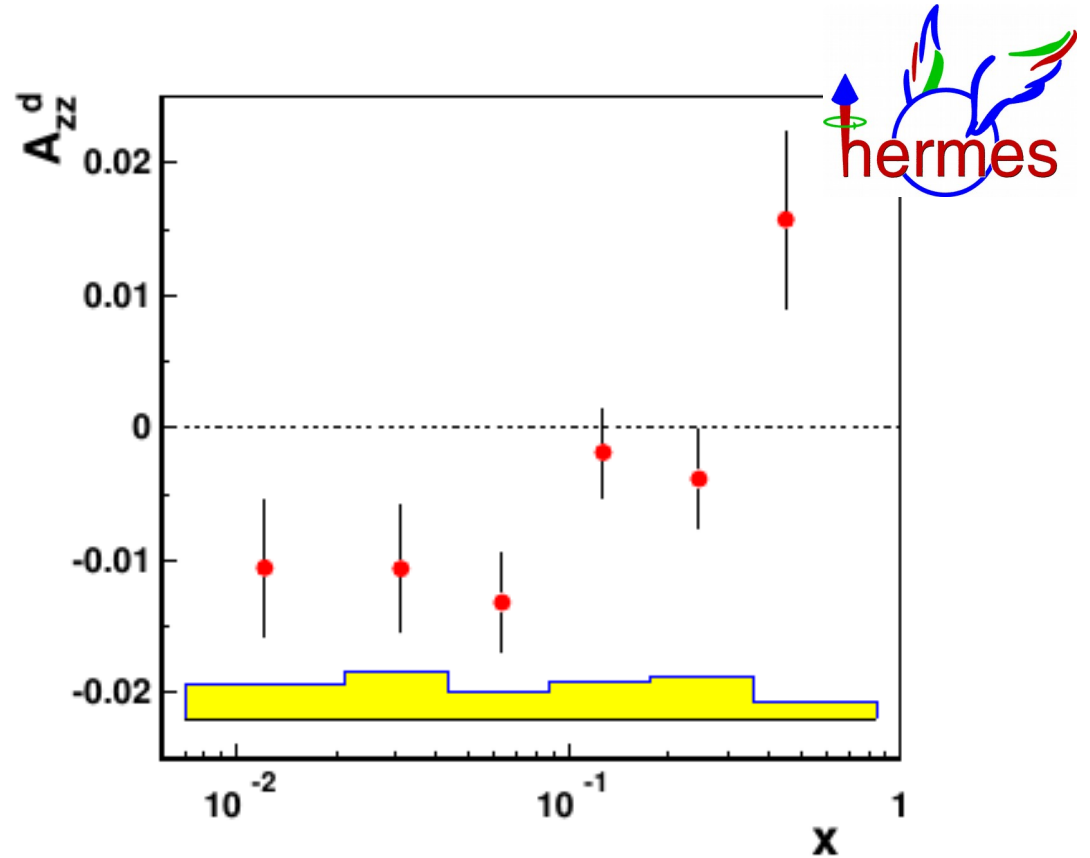
where q^m is parton distribution function in hadron **spin-m** state.

Extraction of Observable

$$A_{zz} = \frac{2}{fP_{zz}} \frac{\sigma_{\dagger} - \sigma_0}{\sigma_0}$$

$$= \frac{2}{fP_{zz}} \left(\frac{N_{\dagger}}{N_0} - 1 \right)$$

$$T = \frac{N_T}{R_T} = \frac{16}{P_{zz}^2 f^2 \delta A_{zz}^2 R_T}$$



Atomic-gas target

σ_{\dagger} : Tensor Polarized cross-section

σ_0 : Unpolarized cross-section

P_{zz} : Tensor Polarization

	Hermes	JLAB
P_{zz}	0.8	0.2
Dilution	0.9	0.30
$L(\text{cm}^{-2}\text{s}^{-1})$	10^{31}	10^{35}

$$b_1 = -\frac{3}{2} F_1^d A_{zz}$$

Extraction of Observable

Hermes data show that b_1 is not as small as the prediction for the S-D mixture proposal

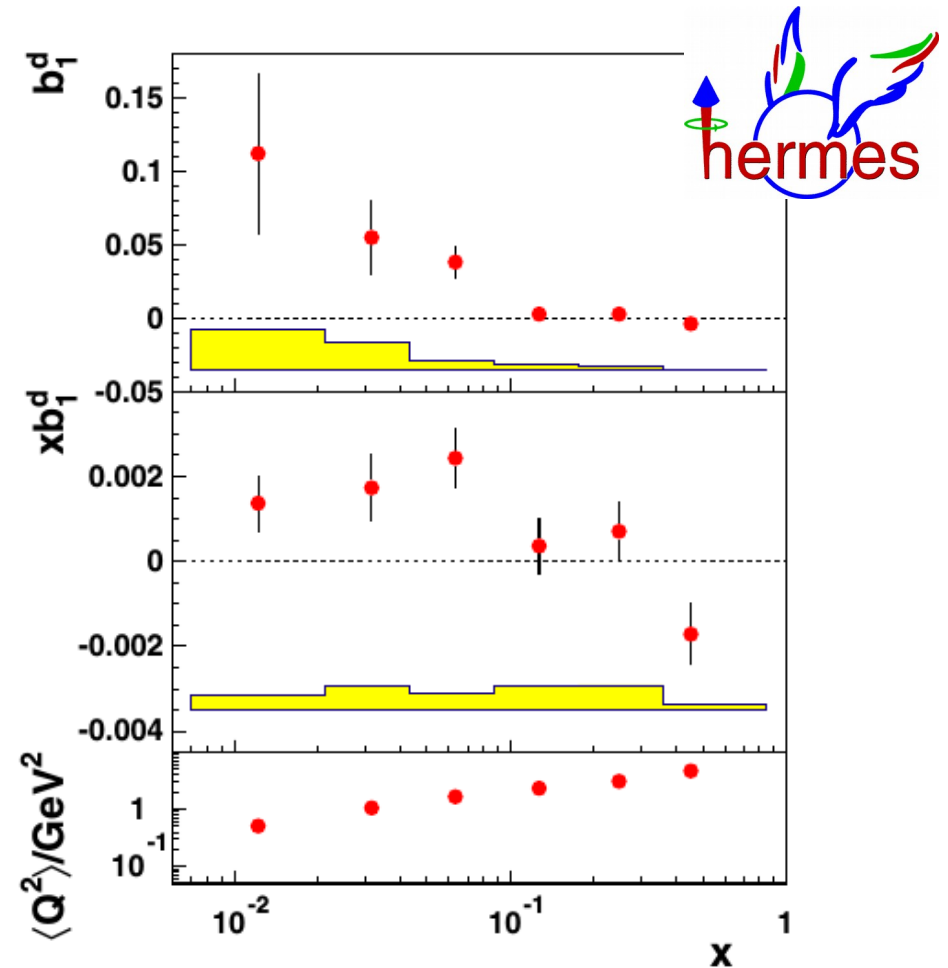
$$xb_1 \sim 10^{-4}$$

↕ **Order of magnitude difference**

$$xb_1 \sim 10^{-3} \text{ in HERMES data}$$

$$\int_{0.002}^{0.85} b_1(x) dx = [1.05 \pm 0.34(\text{stat}) \pm 0.35(\text{sys})] \times 10^{-2}$$

$$\int_{0.02}^{0.85} b_1(x) dx = [0.35 \pm 0.10(\text{stat}) \pm 0.18(\text{sys})] \times 10^{-2}$$



$$b_1 = -\frac{3}{2} F_1^d A_{zz}$$

Extraction of Observable

$$A_{zz} = \frac{2}{fP_{zz}} \frac{\sigma_{\dagger} - \sigma_0}{\sigma_0}$$

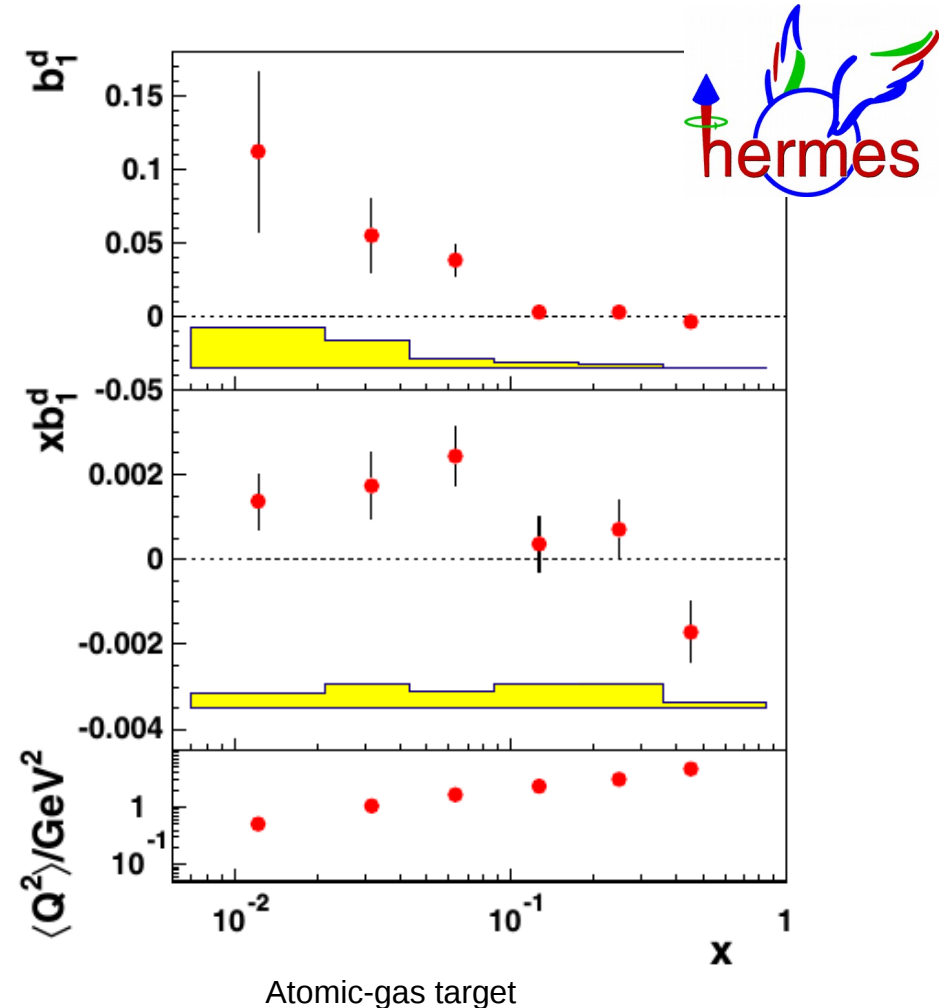
$$= \frac{2}{fP_{zz}} \left(\frac{N_{\dagger}}{N_0} - 1 \right)$$

$$T = \frac{N_T}{R_T} = \frac{16}{P_{zz}^2 f^2 \delta A_{zz}^2 R_T}$$

σ_{\dagger} : Tensor Polarized cross-section

σ_0 : Unpolarized cross-section

P_{zz} : Tensor Polarization



	Hermes	JLAB
P_{zz}	0.8	0.2
Dilution	0.9	0.30
$L(\text{cm}^{-2}\text{s}^{-1})$	10^{31}	10^{35}

$$b_1 = -\frac{3}{2} F_1^d A_{zz}$$

Very Unexpected Result

$$\int b_1(x) dx = 0$$

if the sea quark tensor polarization vanishes

$$\int_{0.0002}^{0.85} b_1(x) dx = 0.0105 \pm 0.0034 \pm 0.0035$$

Efremov and Teryaev (1982, 1999)

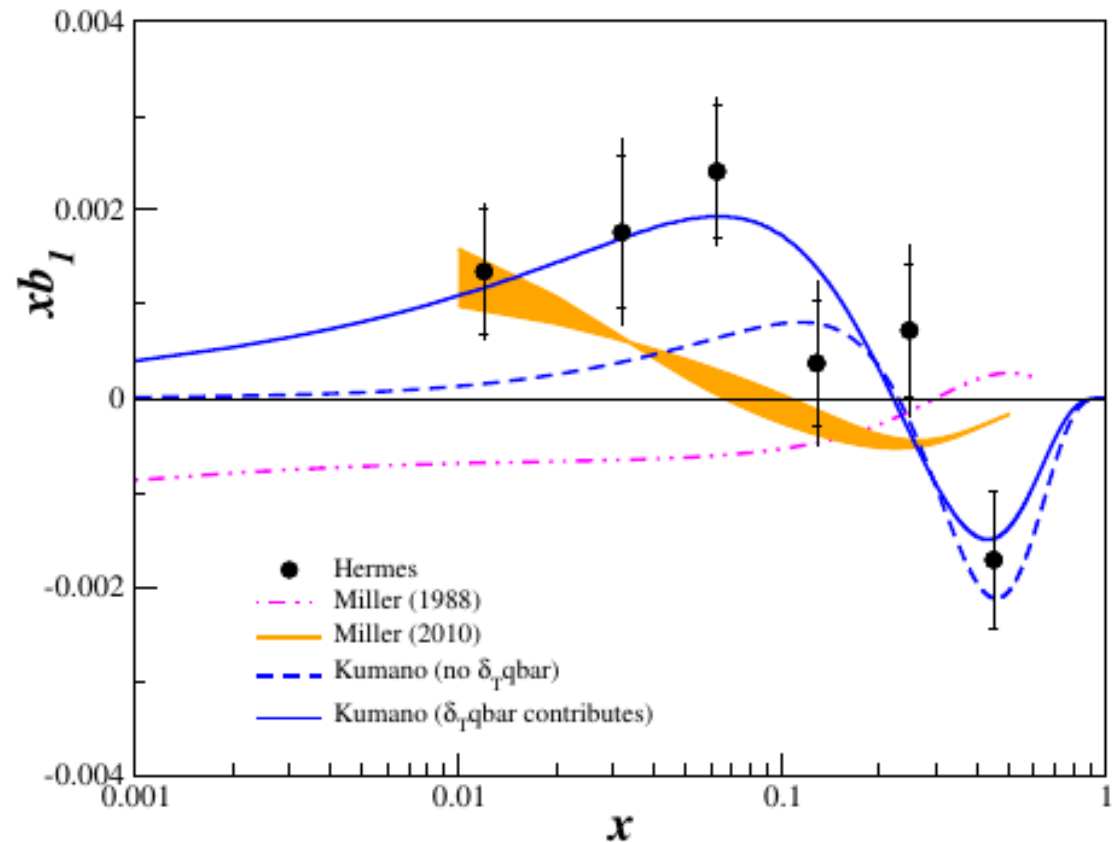
Gluons (spin 1) contribute to both moments

Quarks satisfy the first moment, but

Gluons may have a non-zero first moment!

2nd moment more likely to be satisfied experimentally
since the collective glue is suppressed compared to the sea

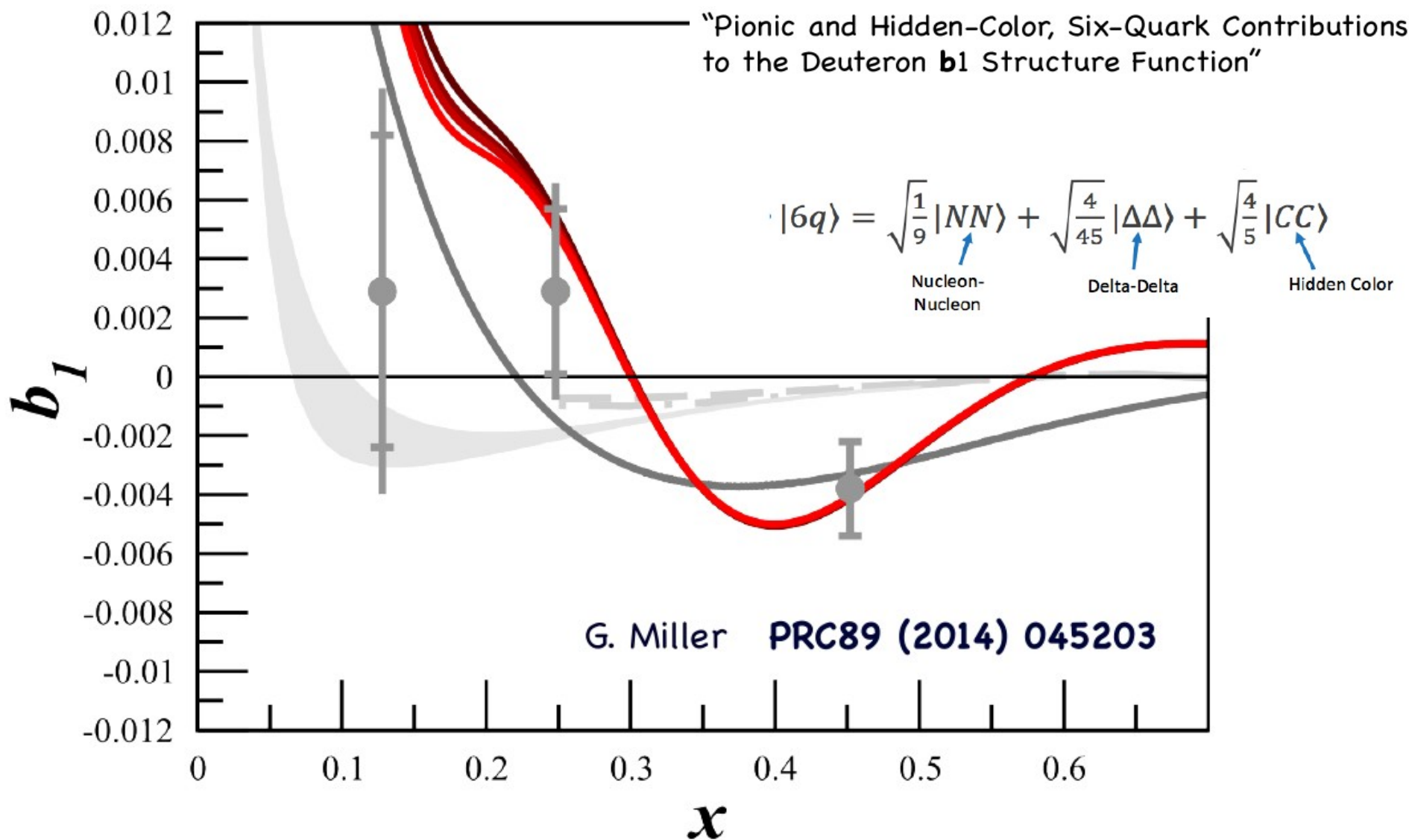
Study of b_1 allows to discriminate between deuteron
components with different spins (quarks vs gluons)



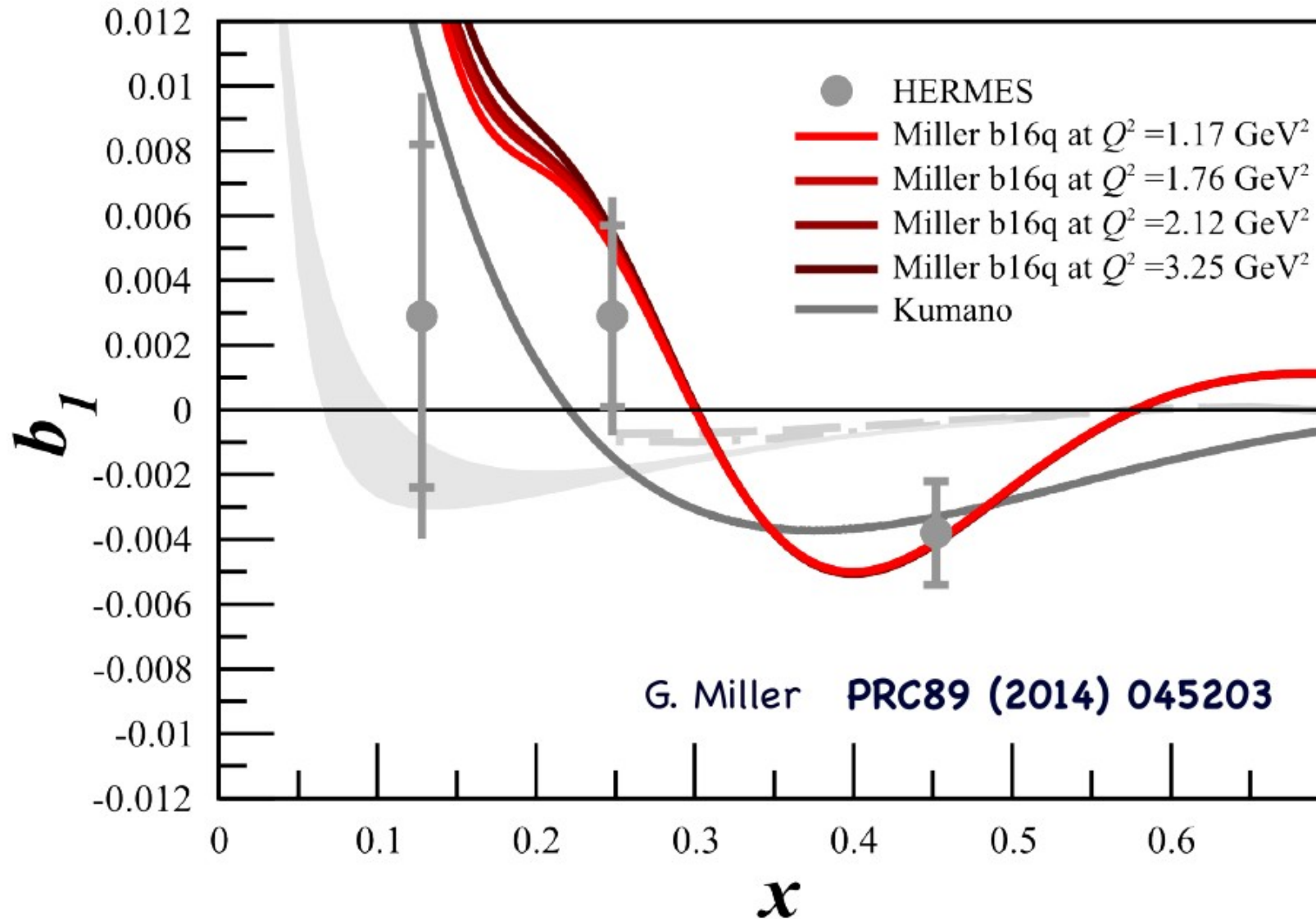
no conventional nuclear mechanism can reproduce the Hermes data

Hidden Color

G. Miller **PRC89 (2014) 045203**



Hidden Color



Systematics

$\delta\xi$

Charge Determination

$< 2 \times 10^{-4}$, mitigated by thermal isolation of BCMs and addition of 1 kW Faraday cup

Luminosity

$< 1 \times 10^{-4}$, monitored by Hall C lumi

Target dilution and length step like changes observable in polarimetry

$< 1 \times 10^{-4}$

Beam Position Drift effect on Acceptance

$< 1 \times 10^{-4}$ (we can control the beam to 0.1 mm, raster over 2cm diameter)

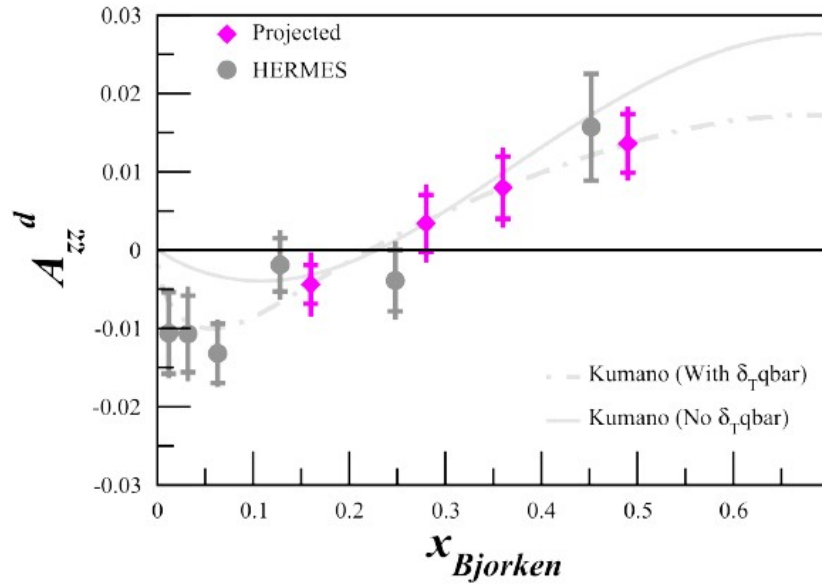
Effect of using polarized beam

$< 2.2 \times 10^{-5}$, using parity feedback

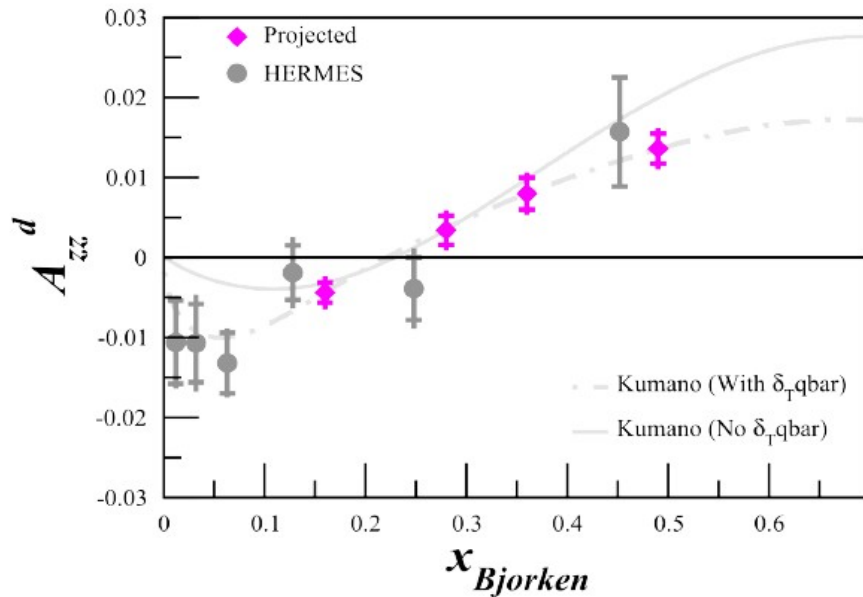
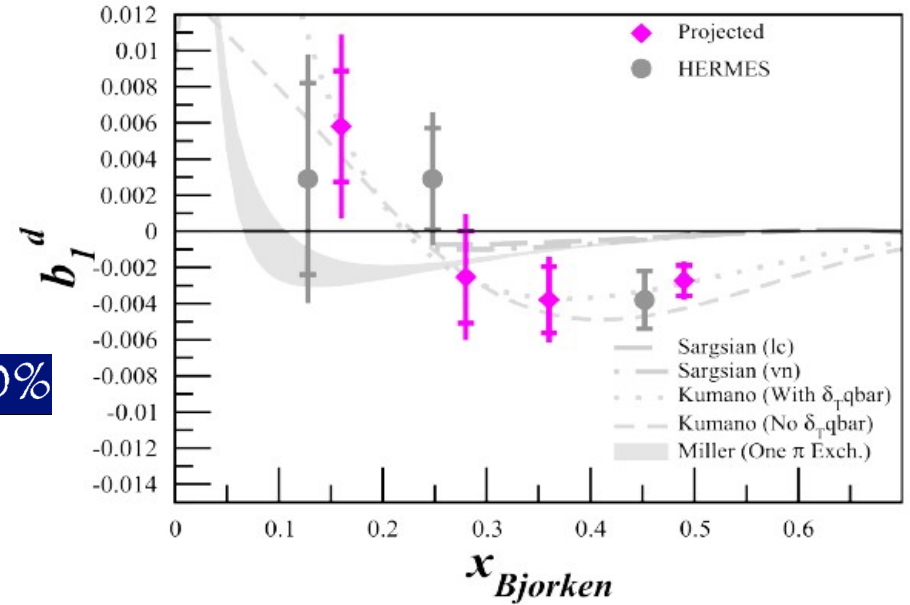
Impact on the observable

$$\delta A_{zz} = \pm \frac{2}{f P_{zz} \sqrt{N_{cycles}}} \delta\xi$$

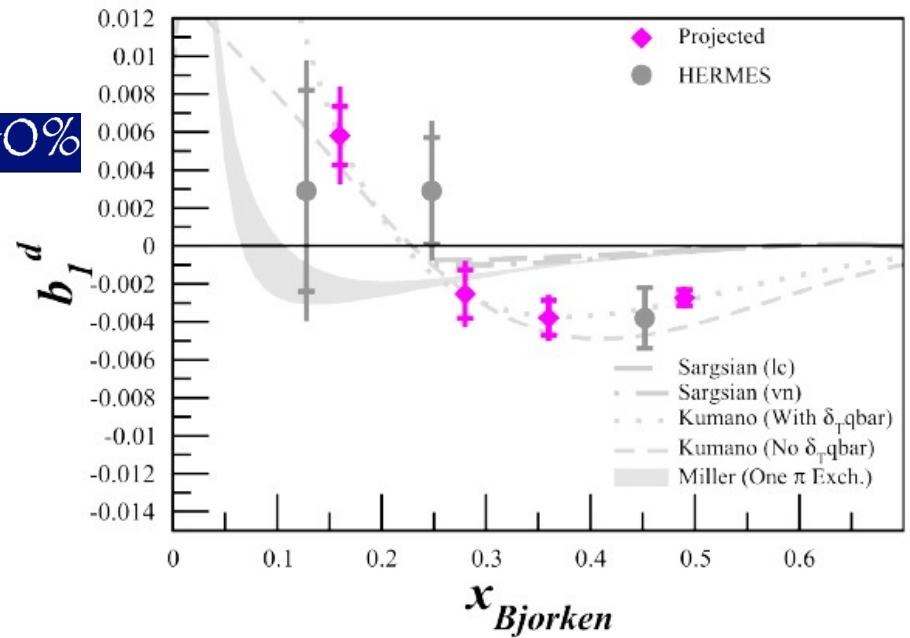
Projected Results



$P_{ZZ} \approx 20\%$



$P_{ZZ} \approx 40\%$



The DY Effort

- 2010 First Discussion with Kumano
 - Possibility of DY access [PRD 59 \(1999\) 094026](#)
[PRD 60 \(1999\) 054018](#)
- Sparked Interest
 - S. Kumano, S. Phys.Rev. D82 (2010) 017501
 - S. Kumano 2014 J. Phys.: Conf. Ser. 543 012001
 - S. Kumano et al. Phys.Rev. D94 (2016) no.5, 054022
 - S. Kumano arXiv:1702.01477
 - S. Kumano arXiv:1902.04712

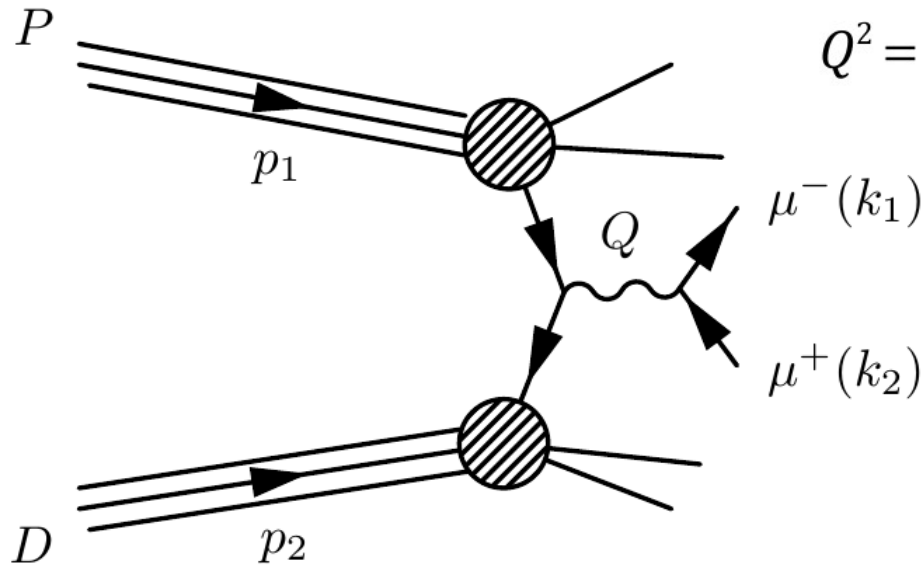
Drell-Yan Process

$$P + D \rightarrow \gamma^* \rightarrow \mu^- \mu^+ + X$$

$$E_p = 120 \text{ GeV}$$

$$s = (p_1 + p_2)^2 = M_p^2 + M_d^2 + 2M_d E_p$$

$$Q^2 = x_1 x_2 s$$



$$W_{\mu\nu} = \int \frac{d^4 \xi}{(2\pi)^4} e^{iQ\xi} \left\langle P_1 S_1 P_2 S_2 \left| J_\mu(0) J_\nu(\xi) \right| P_1 S_1 P_2 S_2 \right\rangle$$

DY-Tensor Polarization

There are 108 structure functions for the hadron tensor of unpolarized proton-polarized deuteron Drell-Yan Process, and the spin asymmetry A_{UQ_0} is measured with the tensor polarized deuteron.

$$A_{UQ_0} = \frac{1}{2\langle\sigma\rangle} \left[\sigma(\bullet, 0) - \frac{\sigma(\bullet, +1) + \sigma(\bullet, -1)}{2} \right]$$

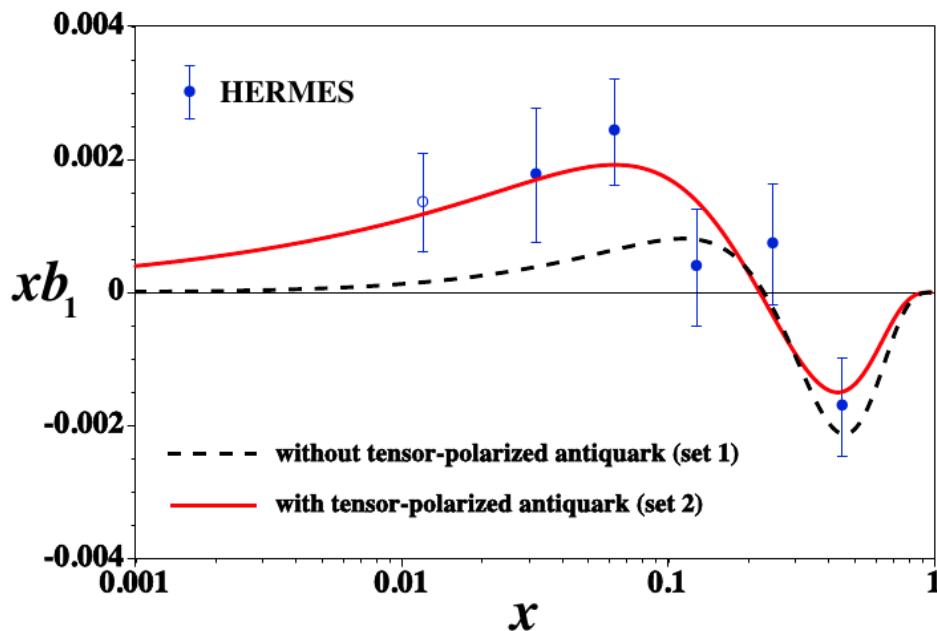
PRD 59 (1999) 094026
PRD 60 (1999) 054018

In Parton Model

$$A_{UQ_0} = \frac{\sum_i e_i^2 (q_i(x_1) \delta_T \bar{q}_i(x_2) + \bar{q}_i(x_1) \delta_T q_i(x_2))}{2 \sum_i e_i^2 (q_i(x_1) \bar{q}_i(x_2) + \bar{q}_i(x_1) q_i(x_2))}$$

Update to Model

The spin asymmetry A_{UQ0} will indicate that existence of tensor-polarized distributions $\delta_T q$ and $\delta_T \bar{q}$, which are only available in D-wave deuteron. In experiment, the tensor-polarized distributions have been confirmed by **Hermes** measurements for b_1 of electron-deuteron DIS.

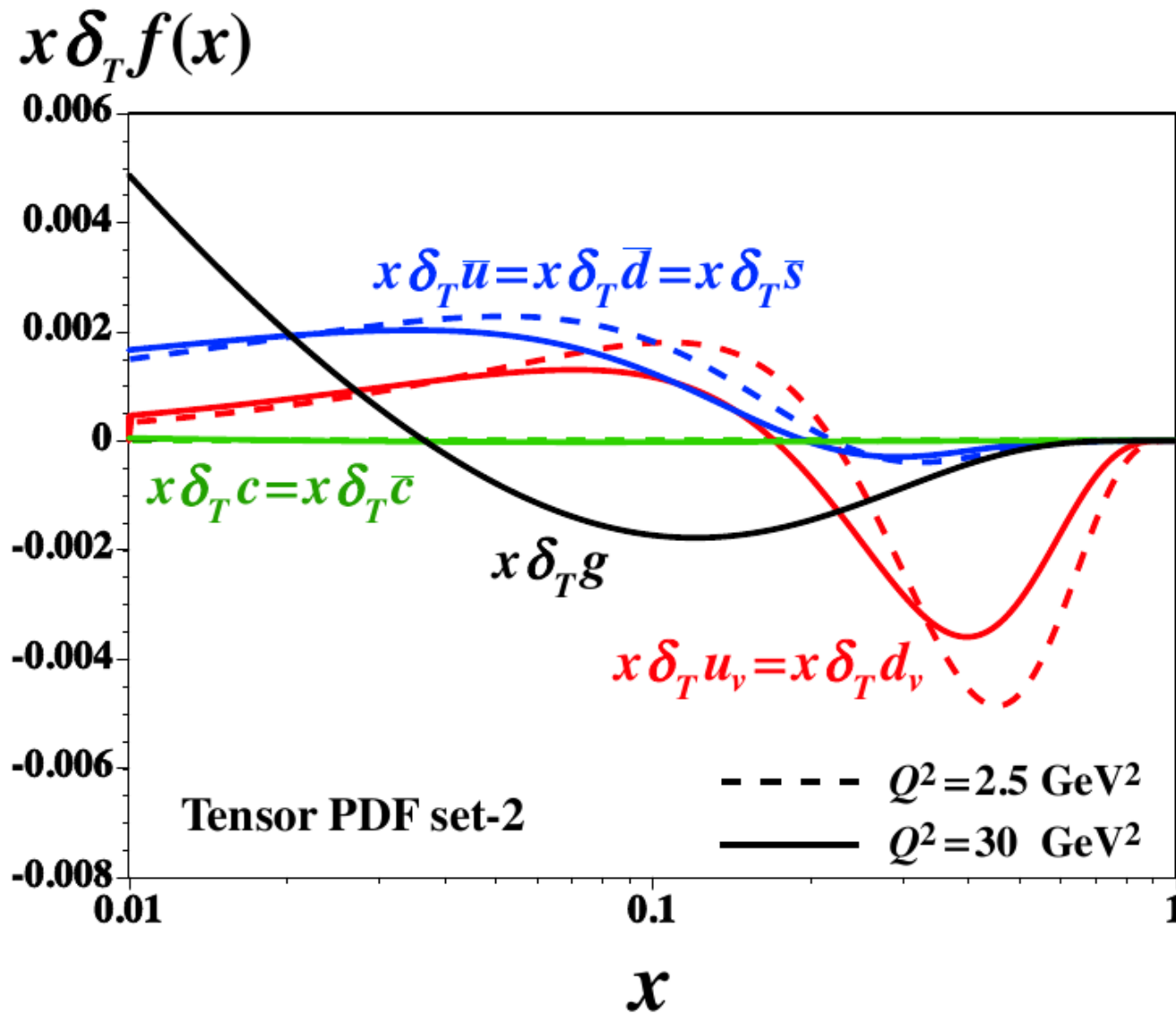


Set-1 results of xb_1 can not explain the Hermes data at small x ($x < 0.1$).

Set-2 results can fit the data well enough.

It is better to consider the antiquark tensor-polarized distributions at $Q^2 = 2.5 \text{ GeV}^2$.

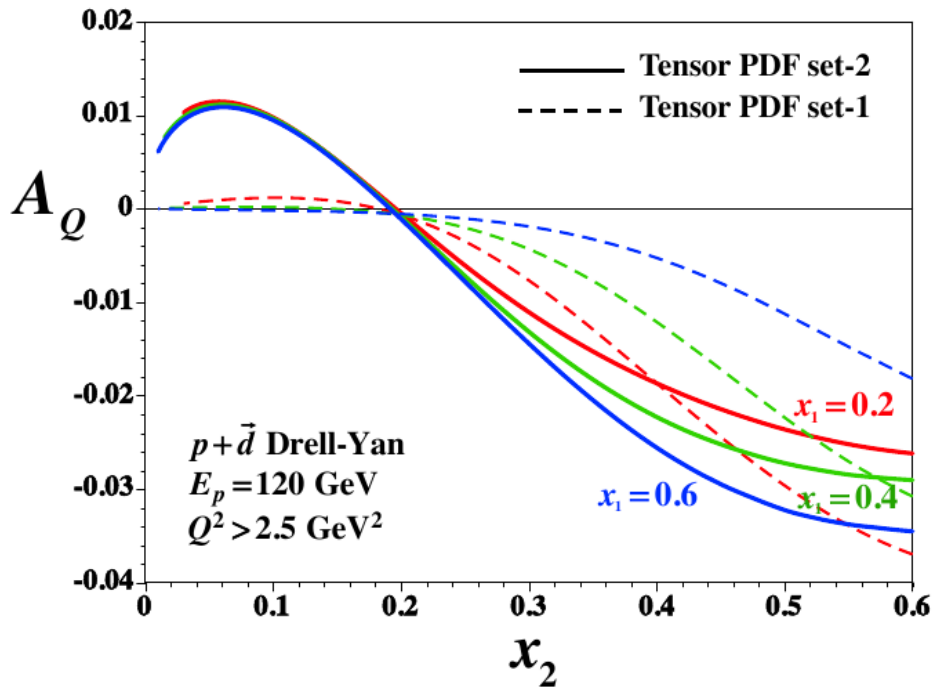
Update to Model



symmetry for antiquarks

$$\delta_T \bar{u} = \delta_T \bar{d} = \delta_T \bar{s} \neq \delta_T \bar{c}$$

Update to Model



In the figure, tensor-polarized asymmetry A_Q is shown at typical values of $x_1 = 0.2, 0.4$ and 0.6 .

$$A_Q(x_1, x_2) = 2A_{UQ_0}(x_1, x_2)$$

$$A_{UQ_0} = \frac{\sum_i e_i^2 (q_i(x_1) \delta_T \bar{q}_i(x_2) + \bar{q}_i(x_1) \delta_T q_i(x_2))}{2 \sum_i e_{ii}^2 (q_i(x_1) \bar{q}_i(x_2) + \bar{q}_i(x_1) q_i(x_2))}$$

The values of set-1 and set-2 are both **a few percent**.

The set-1 results are so different from those of set-2 at small region of x_2 , and this is because that **antiquark tensor-polarized distributions** are more important when x_2 is small.

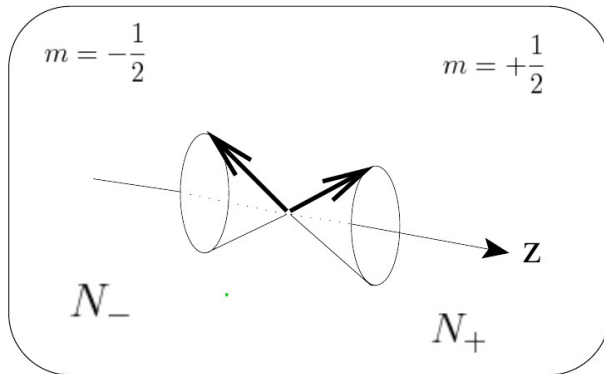
The set-2 results should be **more reliable**, since the tensor-polarized distributions can also explain the Hermes data well.

Forward

The new structure function b_1 (DIS) and spin asymmetry A_Q (Drell-Yan) of deuteron reflect the tensor-polarized distributions, which have a close relationship with the orbital angular momentum in spin-1 hadrons. In this talk, we give the theoretical estimate of the spin asymmetry A_Q , and it is of the order of a few percent. In the future, those quantities could be measured by Jlab (b_1) and Fermilab (A_Q), which may reveal the puzzle of deuteron.

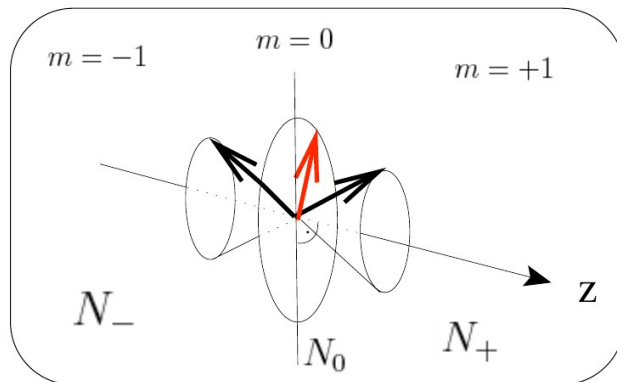
Tensor Polarization

Spin-1/2 system in B-field leads to 2 sublevels due to Zeeman interaction



$$P_z = \frac{N_+ - N_-}{N_+ + N_-}$$

$$-1 < P_z < +1$$



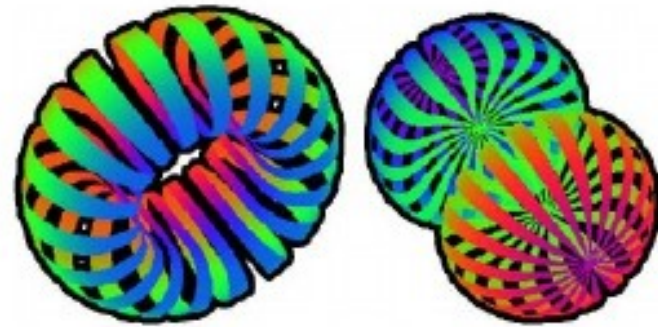
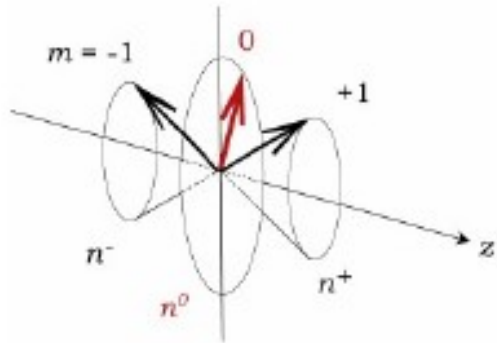
$$P_z = \frac{N_+ - N_-}{N_+ + N_-}$$

$$P_{zz} = \frac{(N_+ - N_0) - (N_0 - N_-)}{N_+ + N_0 + N_-} = \frac{(N_+ + N_-) - 2N_0}{N_+ + N_0 + N_-}$$

For Spin-1 Target

- Three magnetic sublevels
- Two transitions $+1 \rightarrow 0$ and $0 \rightarrow -1$
- Deuteron electric dipole moment eQ
- Interaction with electric field gradient

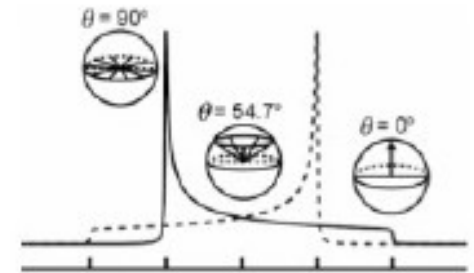
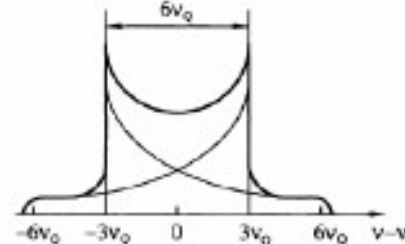
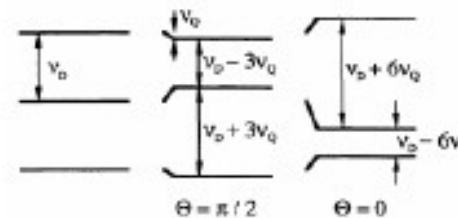
Novel Targets for Novel Physics



Densities of the deuteron in its two spin projections $I_z = 0$ and $I_z = 1$

$$P = \frac{n_+ - n_-}{n_+ + n_- + n_0} \quad (-1 < P_z < 1)$$

$$P_{zz} = \frac{n_+ - 2n_0 + n_-}{n_+ + n_- + n_0} \quad (-2 < P_{zz} < 1)$$

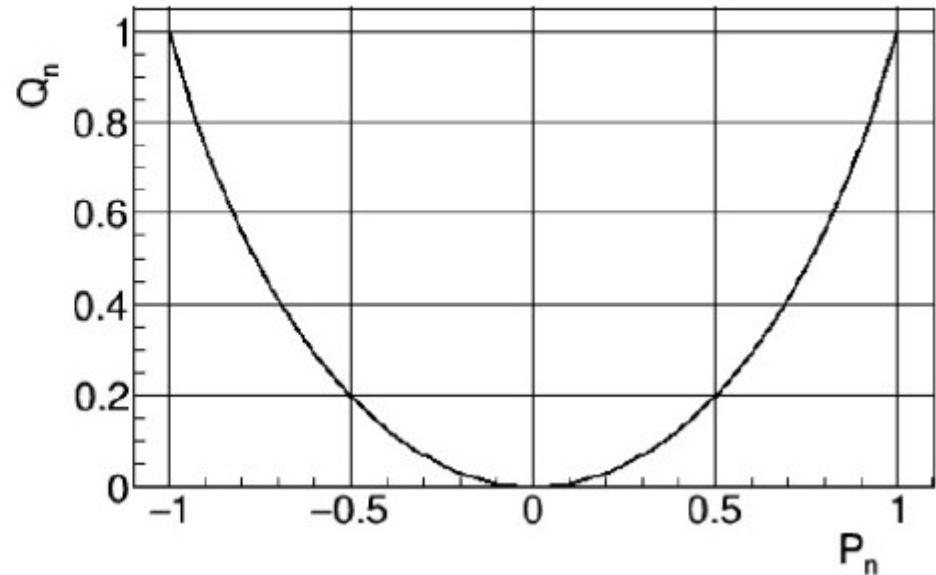
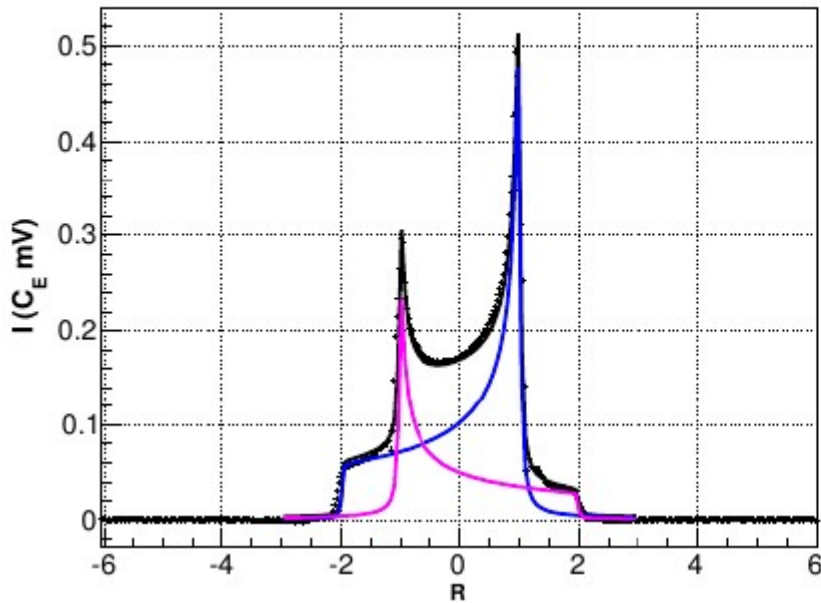


- Using Spin-1 (ND_3) Target
- Three Magnetic substates (+1,0,-1)
- Two Transitions (+1 \rightarrow 0) and (0 \rightarrow -1)
- Deuterons electric quadrupole moment eQ
- Interacts with electric field gradients within lattice

Options of Enhancement

- Increase the B-Field (Longitudinally Polarized)
- Decrease Temperature
- Manipulate using AFP
- RF CW-NMR Manipulation

Natural Equilibrium Polarization



$$R = \frac{\omega - \omega_d}{3\omega_q}$$

$$P_n = \frac{2\hbar}{g^2 \mu_N^2 \pi N} \int_{-\infty}^{\infty} \frac{3\omega_Q \omega_D}{3R\omega_Q + \omega_D} \chi''(R) dR$$

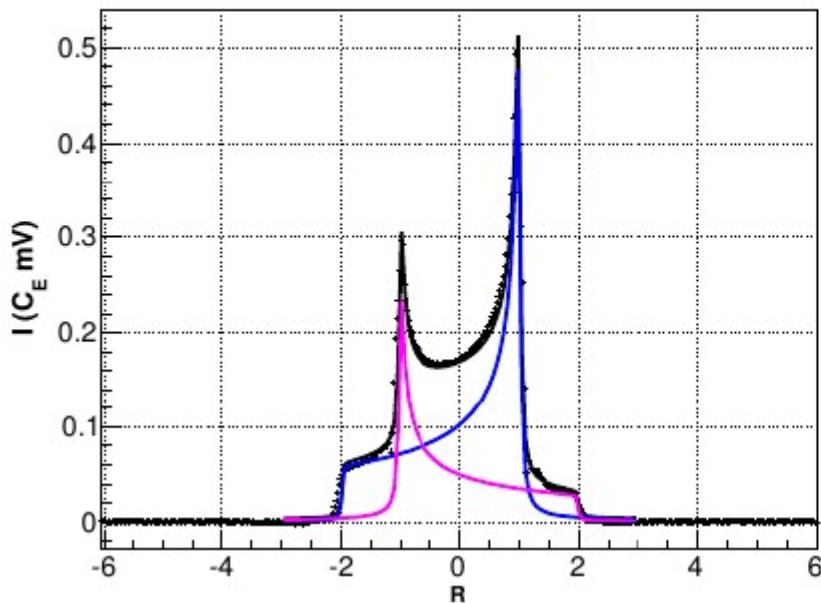
$$= \frac{1}{C_E} \int_{-\infty}^{\infty} I_+(R) + I_-(R) dR,$$

$$Q_n = (I_+ - I_-)/C_E$$

$$Q_n = 2 - \sqrt{4 - 3P_n^2}$$

- Under Boltzmann equilibrium the relationship between vector and tensor polarization always exists
- Under this same condition the Height of each peak maintains a relationship to each other that contains all polarization information
- The ratio of the peak intensities can be used to calculate relative population in each magnetic sub-level

Natural Equilibrium Polarization



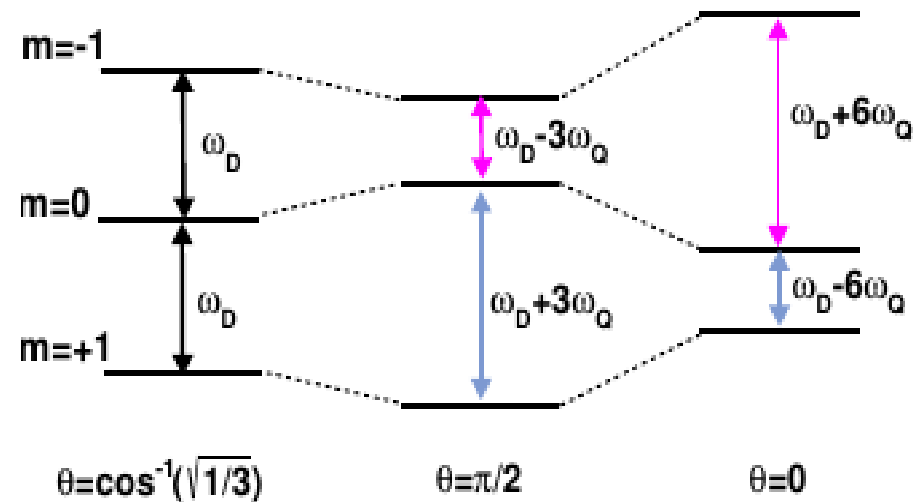
$$R = \frac{\omega - \omega_d}{3\omega_q}$$

$$P_n = \frac{2\hbar}{g^2 \mu_N^2 \pi N} \int_{-\infty}^{\infty} \frac{3\omega_Q \omega_D}{3R\omega_Q + \omega_D} \chi''(R) dR$$

$$= \frac{1}{C_E} \int_{-\infty}^{\infty} I_+(R) + I_-(R) dR,$$

$$Q_n = (I_+ - I_-) / C_E$$

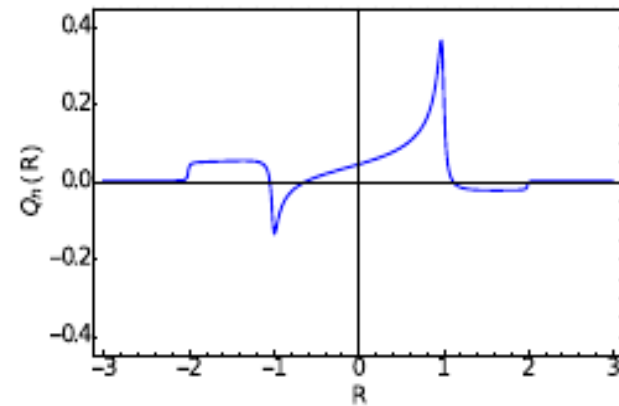
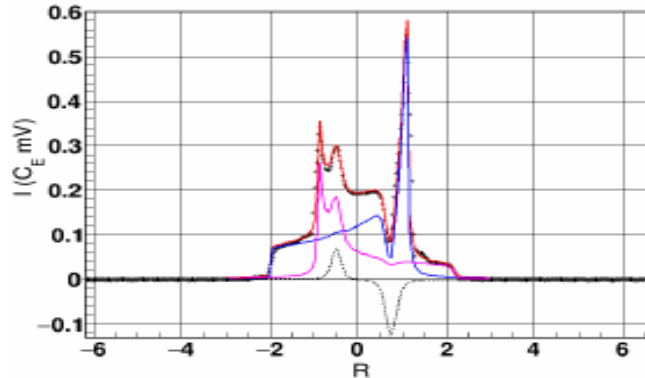
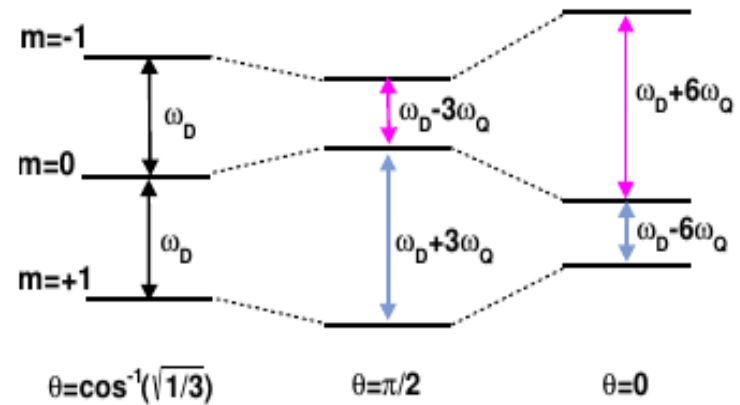
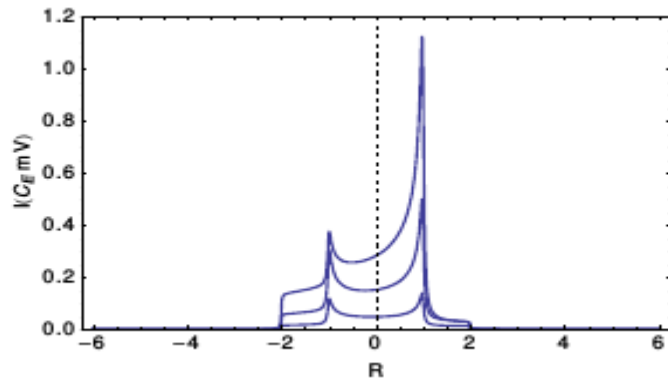
$$= (a_+ - a_0) - (a_0 - a_-)$$



$$Q_n = 2 - \sqrt{4 - 3P_n^2}$$

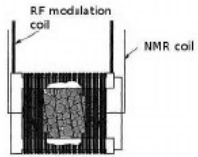
- Under Boltzmann equilibrium the relationship between vector and tensor polarization always exists
- Under this same condition the Height of each peak maintains a relationship to each other that contains all polarization information
- The ratio of the peak intensities can be used to calculate relative population in each magnetic sub-level

Selective Semi-saturation

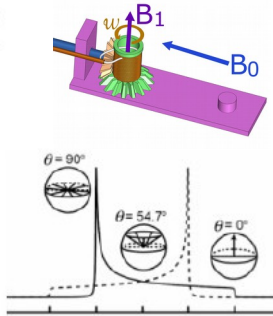
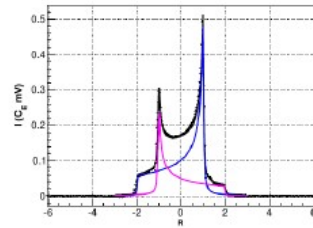
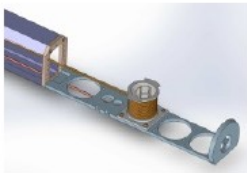


- Selective RF manipulation of the CW-NMR line
- Enhanced by mitigating the amplitudes below zero
- Can be implemented in parallel to DNP

Novel Targets for Novel Physics



RF Manipulation

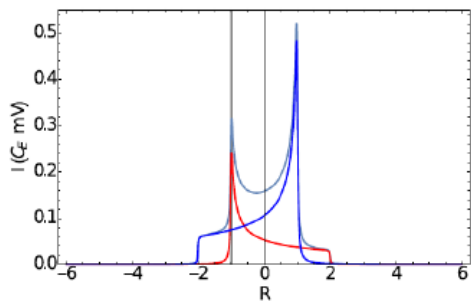


- RF irradiation at the Larmor frequency induces transitions between $m=0$ and other energy levels
- RF induced transitions at a single θ has a resulting effect on two positions in the line R and $-R$ through conservation of energy
- This can be implemented to shrink one transition lines area and enhancing the other resulting in tensor polarization manipulation

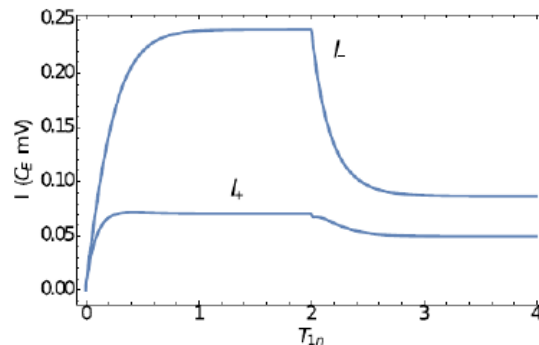
- Study Optimization Analytically
- Develop Simulated Lineshape under RF
 - Empirical info from RF-power profile and Spectral diffusion
 - Rate Eq for overlap ratio
 - Generate theoretical lineshape manipulated by RF
- Develop fitting procedure for measurement
 - Unique constraints for overlapping regions are provided by MC
 - Fit semi-saturated (optimized d-Ammonia)
 - Test measurements with specialized NMR and scattering experiments
- Further Optimized Enhancement
 - Slow Perpendicular Rotation with semi-saturating RF
 - Heavily Reliant on MC for measurements
 - Tested with d-but. but not yet for ammonia

Novel Tensor Enhanced Target

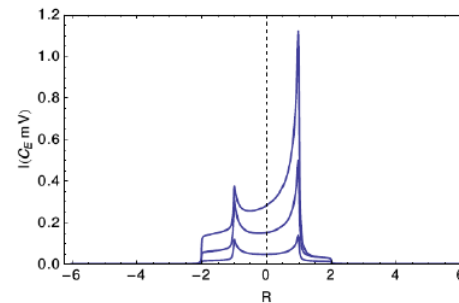
Tensor Enhancement Mechanism for single position



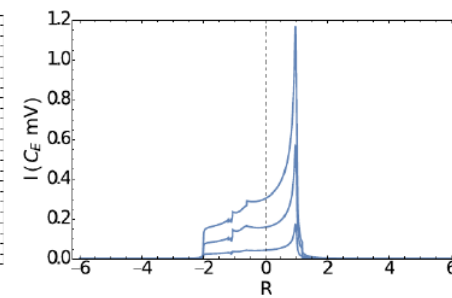
Selective Semi-saturation : Use power appropriate for position optimizing tensor polarization for all R



For peak Semi-saturation significant enhancement occurs by reduction of negative tensor polarization at R as well as adding to positive tensor polarization at $-R$

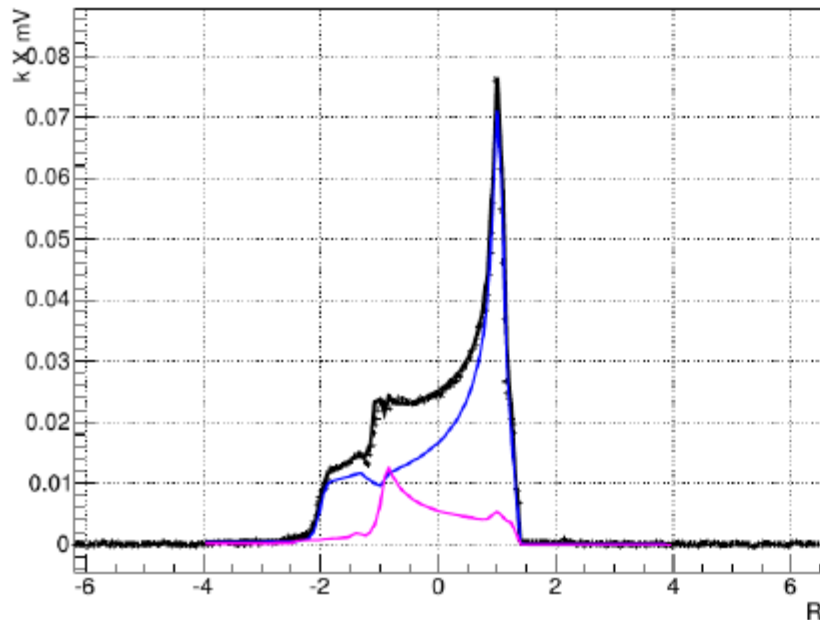


Simulated Examples of regular lineshape (13,42,78%)

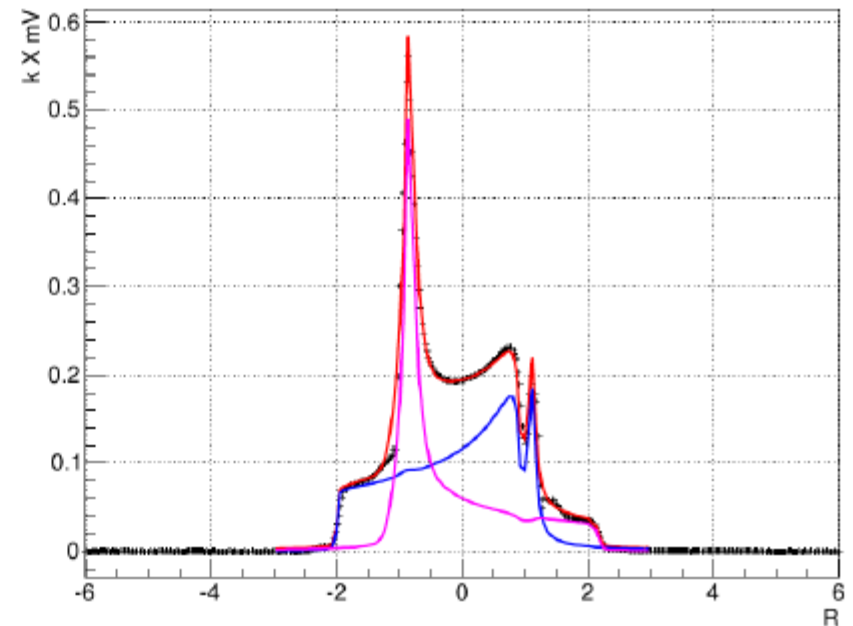


Examples Optimized Tensor Polarization Examples (1.3 \rightarrow 5.4, 13.6 \rightarrow 23.8, 52 \rightarrow 58%)

Selective Semi-saturation (or just hole burning)



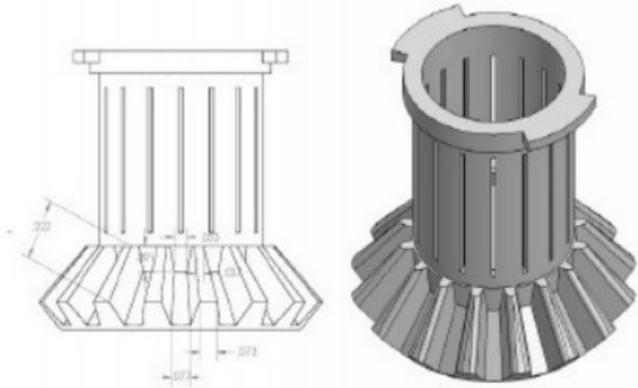
MC overlap with d-but. NMR experimental points (Pn=51 → 45, Qn:20 → 31%)



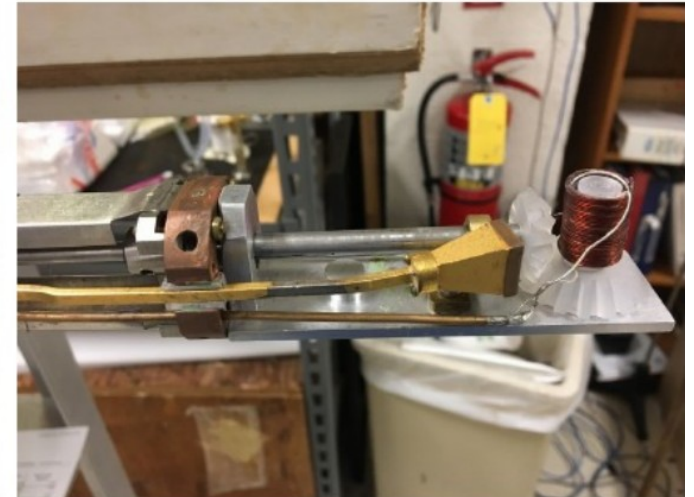
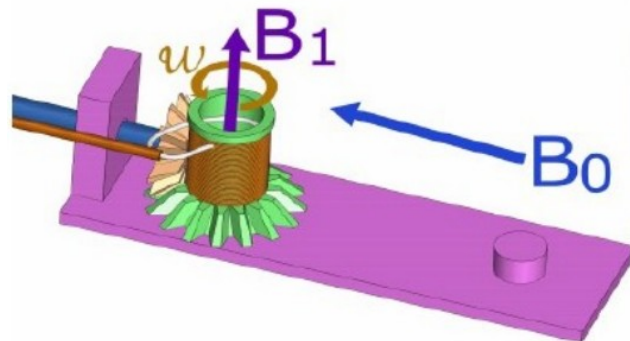
MC with fit and d-but. NMR experimental points (Pn=48 → 46, Qn:18 → 6%)

$$R = \frac{\omega - \omega_d}{3\omega_q}$$

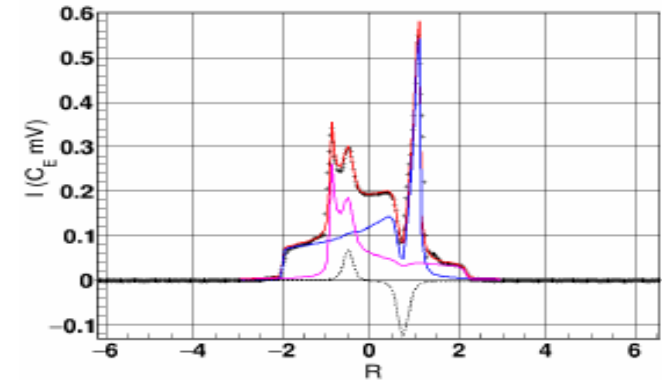
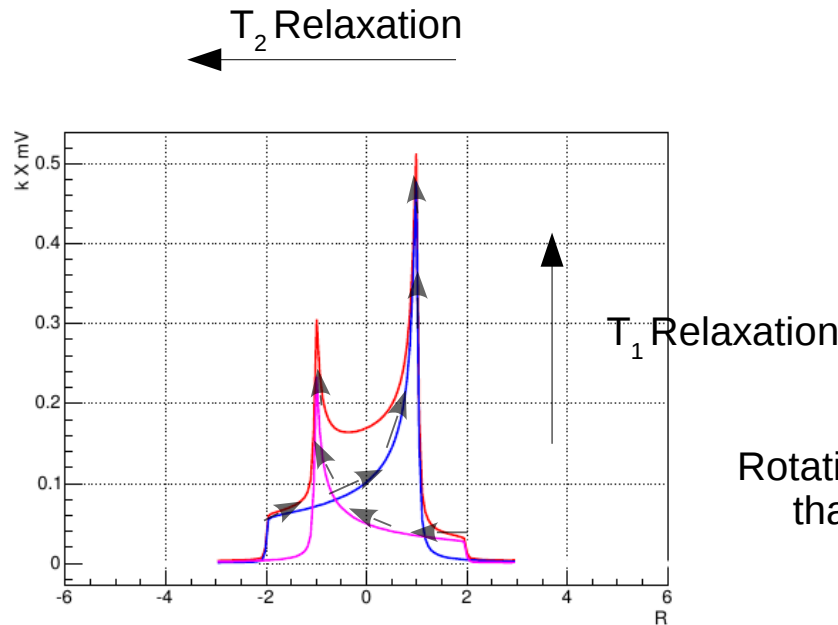
What Things Look Like



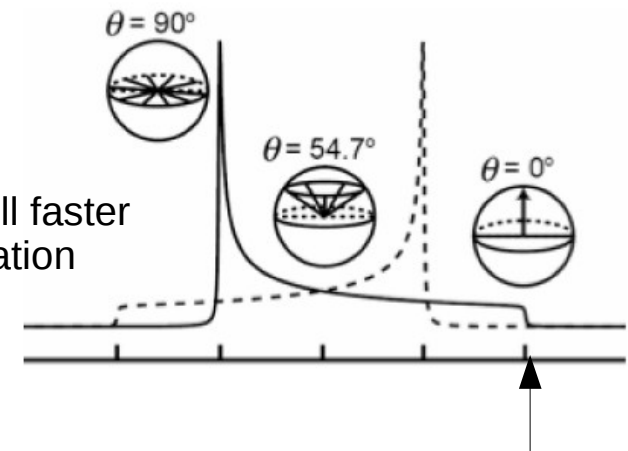
- Kel-F (C_2ClF_3)_n cup and driving gear
- Motor outside cryostat
- NMR coil around cup
- Already used with several designs at UVA
- 1 Hz achieved with no problem
- Fixed beam spot



Rotating Target Concept



Rotational rate still faster than T_2 Relaxation



SSS with slow rotation

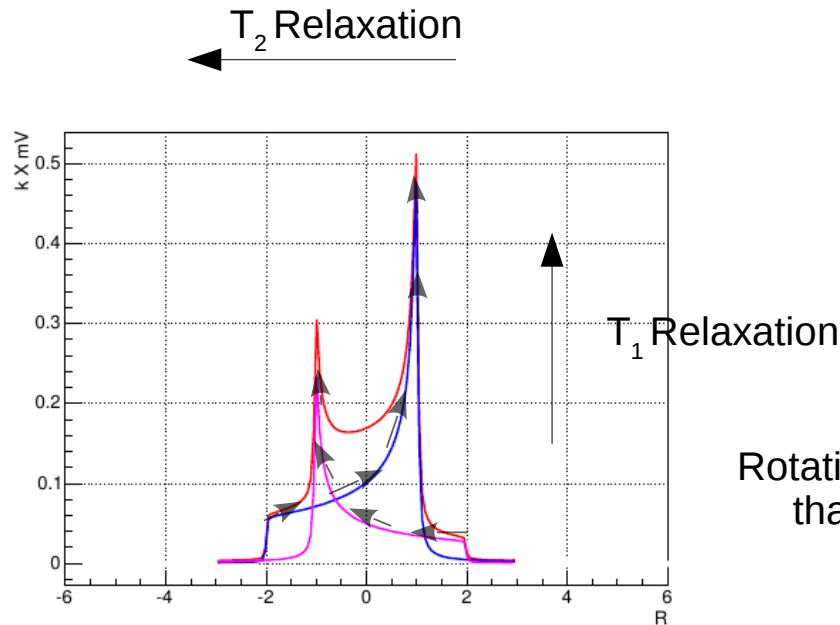
- Selective saturation/pumping while rotating
- Saturated domain moves with rotation
- Can enhance Q or go $-Q$

$$Q_n = (I_+ - I_-) / C_E$$

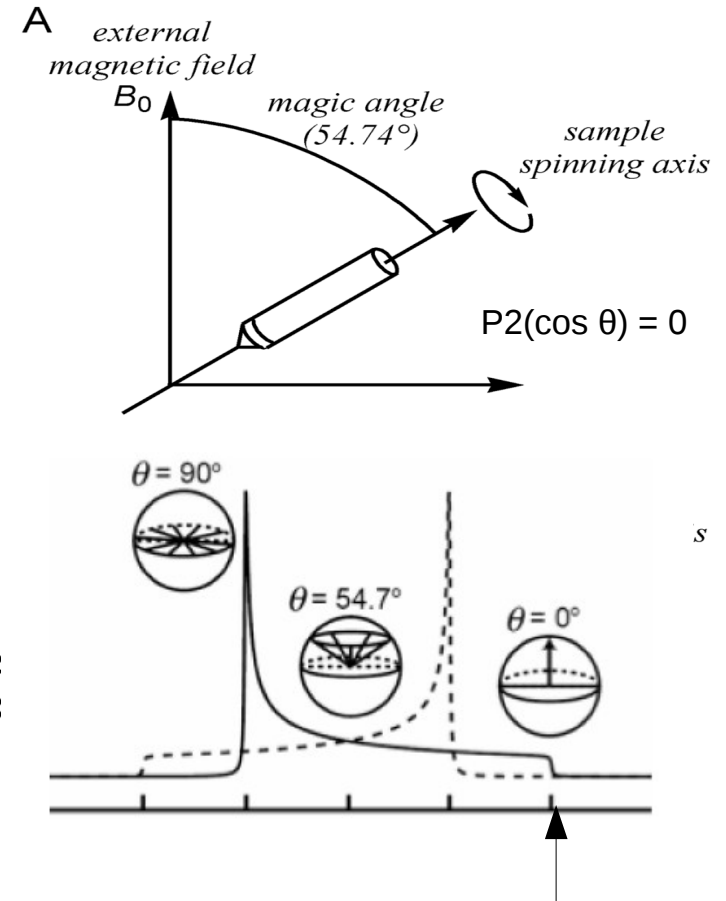
$$= (a_+ - a_0) - (a_0 - a_-)$$

Rotating Target Concept

For dipolar couplings, the principal axis corresponds to the internuclear vector between the coupled spins



Rotational rate :
than T_2 Relaxation



SSS with slow rotation

- Selective saturation/pumping while rotating
- Saturated domain moves with rotation
- Can enhance Q or go -Q

$$Q_n = (I_+ - I_-) / C_E$$

$$= (a_+ - a_0) - (a_0 - a_-)$$

RF-Manipulated Signals

Fast target helicity flips through Adiabatic Fast Passage (AFP)

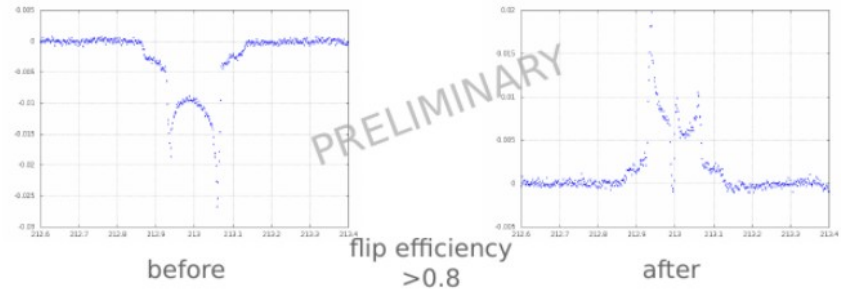
AFP at UVA

performed AFP on different materials (5T, 1K)
 15NH3, D-butanol, butanol+tempo
 preliminary results on flip efficiency

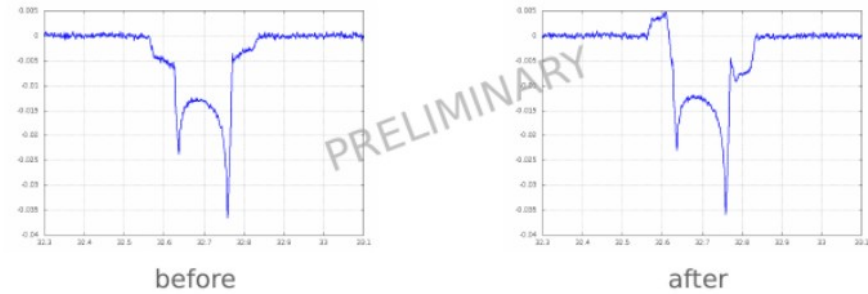
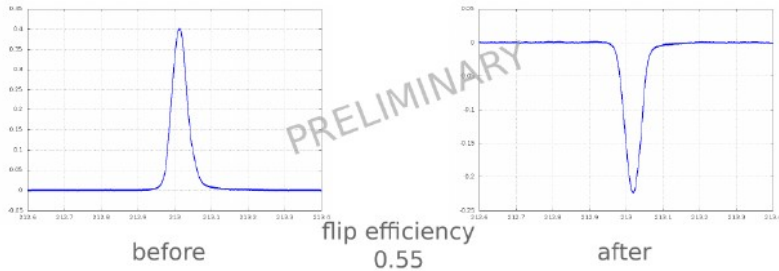
Table 1
 Results from AFP experiments with various nuclei in different target materials

Nuclei	Substance dopant	ϵ^- conc (spins/g)	βP^{max}
^1H	1-butanol EHBA-C(V)	2.0×10^{19}	-0.76
^7Li	^7LiH (irradiated)	low	-1.90 -0.90
^{19}F	8-fluoro-1-pentanol	1×10^{20}	-0.37
^1H	TEMPO		-0.40
^1H	1-butanol- d_{10}	2.36×10^{19}	-0.92
^1H	EHBA-C(V)- d_{22}	6.35×10^{19}	-0.90

NIM 356 (1995) 108

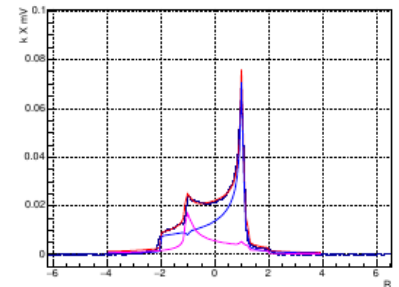
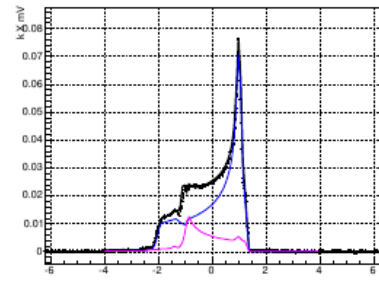
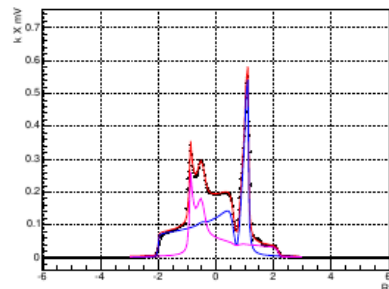
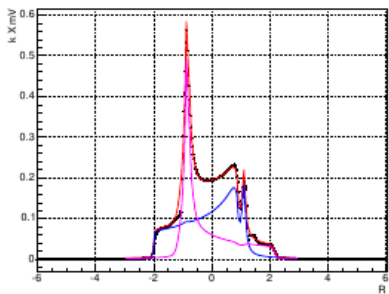


15NH3



AFP produces rotation of the macroscopic magnetization vector by sweeping through resonance in a short time compared to the relaxation time

- Set record for Tensor Polarization for Deuteron (d-b only) $Q > 31\%$ @ 1K 5T
- Set record for AFP flip with Proton $e > 50\%$ @ 1K 5T



Achieved So Far

- Before recent research (1984): ~20%
- Recent studies SSS: (2014-2015): ~30%
- AFP with SSS (2016): ~34%
- Rotation with SSS: ~39%

DK Eur. Phys. J. A (2017) 53: 155

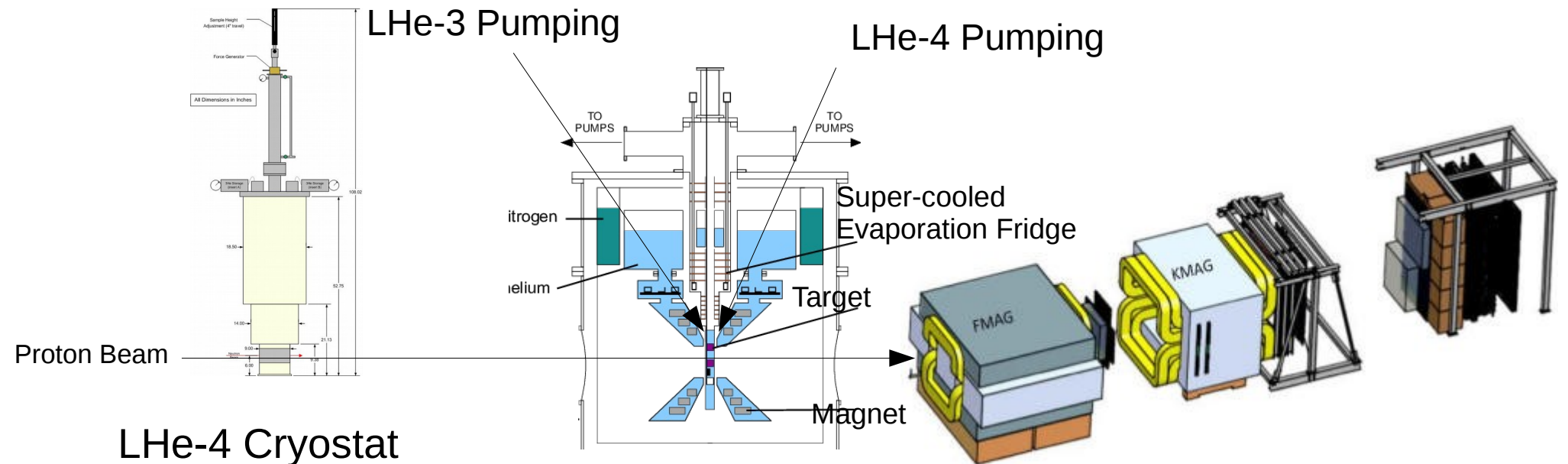
DK PoS, PSTP2015:014 (2016)

DK J.Phys.Conf.Ser., 543(1):012015 (2014)

DK Int.J.Mod.Phys.Conf.Ser., 40(1):1660105 (2016)

A Possible Fermilab Setup

Split Pair



LHe-4 Cryostat

- No Field
- 4 K reservoir
- Hold ND3 with no Polarization

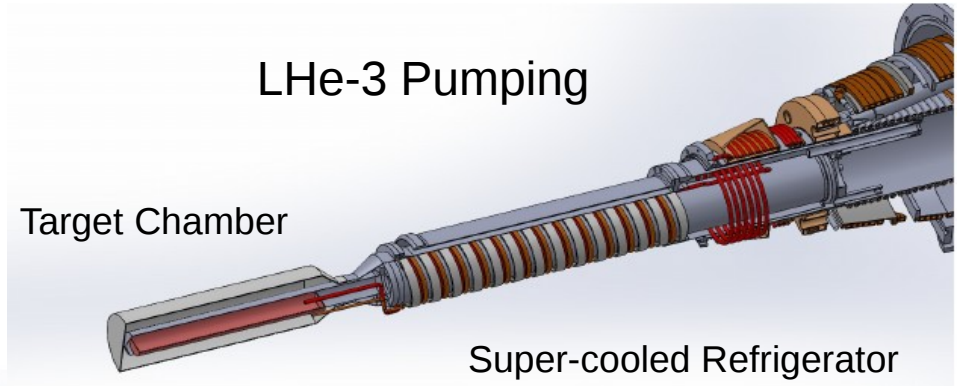
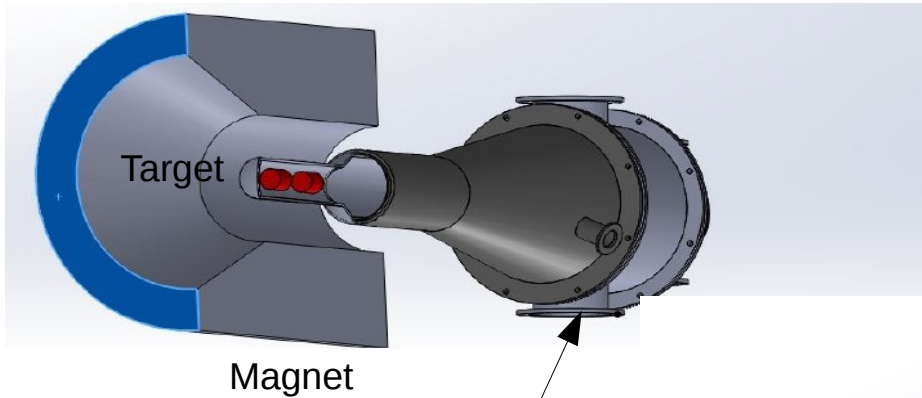
Supercooled He-4 System

- High Cooling Power
- Low Temp 0.4 K
- High ND3 Tensor Polarization ~70%

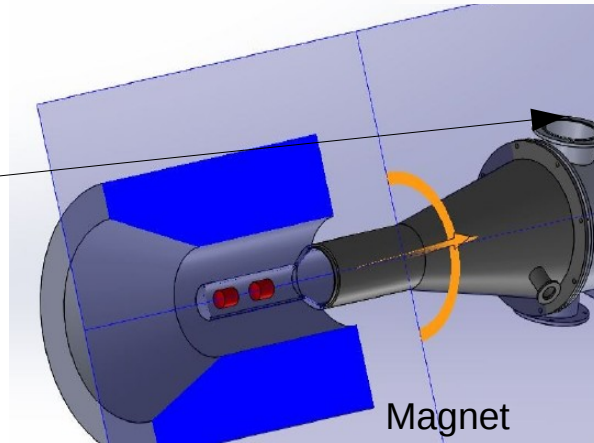
What to Add

- New Magnet
- New Fridge
- He-3 System
- Additional Pumps

A Possible Fermilab Setup



LHe-4 Pumping



LHe-3 Pumping

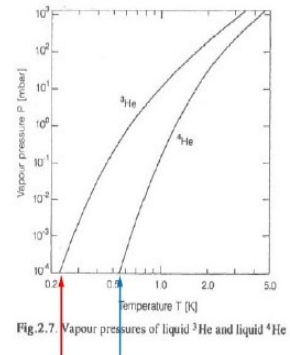
Target Chamber

Super-cooled Refrigerator

$$P \propto \exp\left(-\frac{L}{RT}\right)$$

Latent heat ^4He ~90 J/mol
 Latent heat ^3He ~40 J/mol

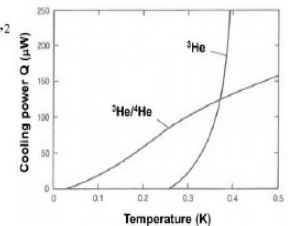
Cooling power: exponentially small at low temperature
 Pumping on ^4He $T \sim 1$ K (normally down to 1.8 K)
 Pumping on ^3He $T \sim 0.26$ K (down to 0.3 K)



^3He - ^4He dilution refrigeration: use the difference of the specific heats of the two phases (the enthalpy of mixing);

$$\Delta H \propto \int \Delta C dT \Rightarrow Q \propto x \Delta H \propto T^2$$

Dilution refrigerator
 cooling power: $\sim T^2$



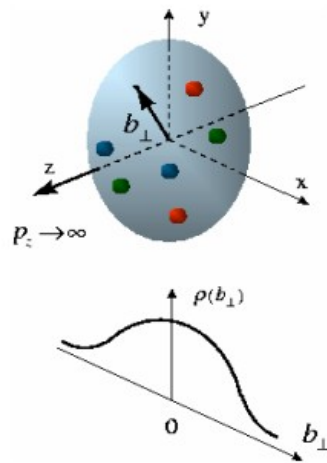
Super-cooled He-4 System

- High Cooling Power
- Low Temp 0.4 K
- High ND3 Tensor Polarization ~70%

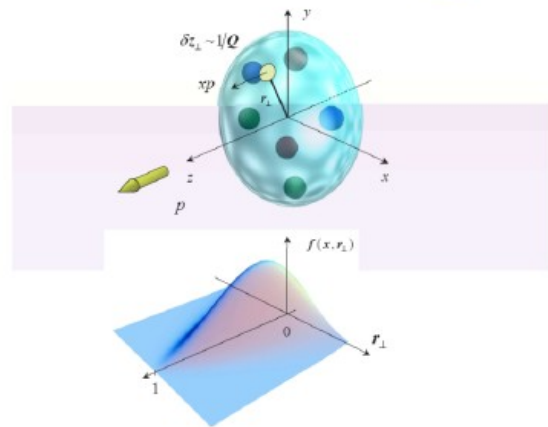
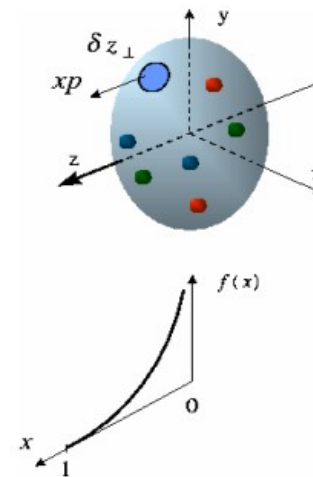
High Cooling Power High Intensity Beams

3D Structure of Nucleon

Form Factors
transverse charge and magnetization
distributions
(GPD integrated over x)



Parton Distributions Functions (PDFs)
longitudinal momentum (DIS)



Generalized Parton Distributions (GPDs)

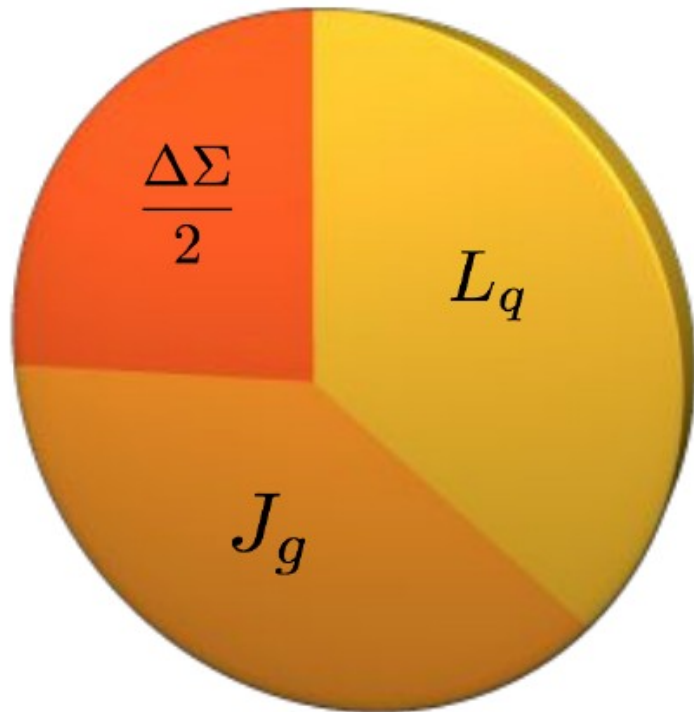
Transverse spatial distribution of quarks with longitudinal momentum fraction x

GPDs “unify” form factors and parton distributions

Shifting Gears

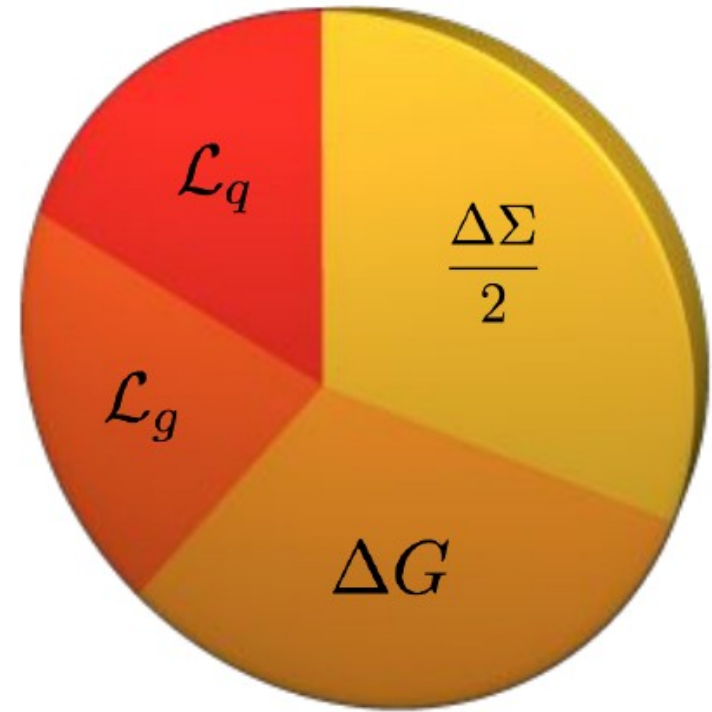
Another Look at OAM

Ji



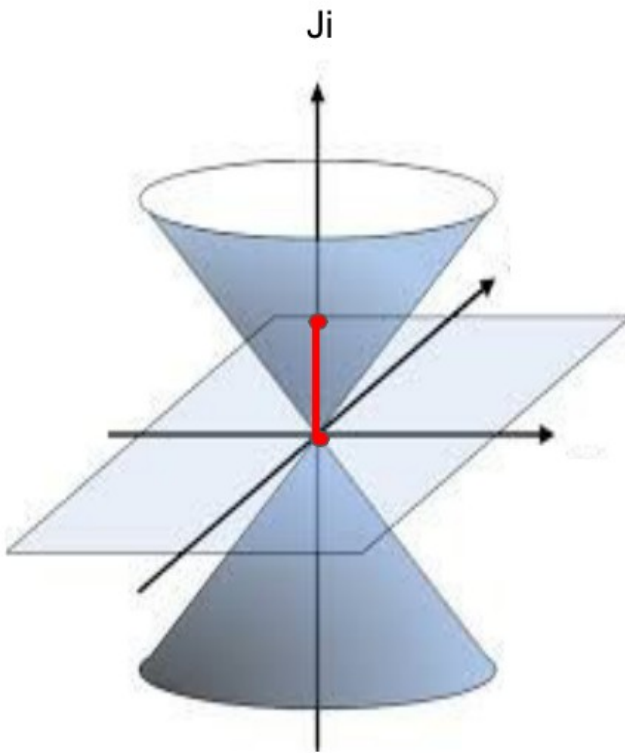
$$\frac{1}{2} = \frac{\Delta\Sigma}{2} + L_q + J_g$$

Jaffe Manohar

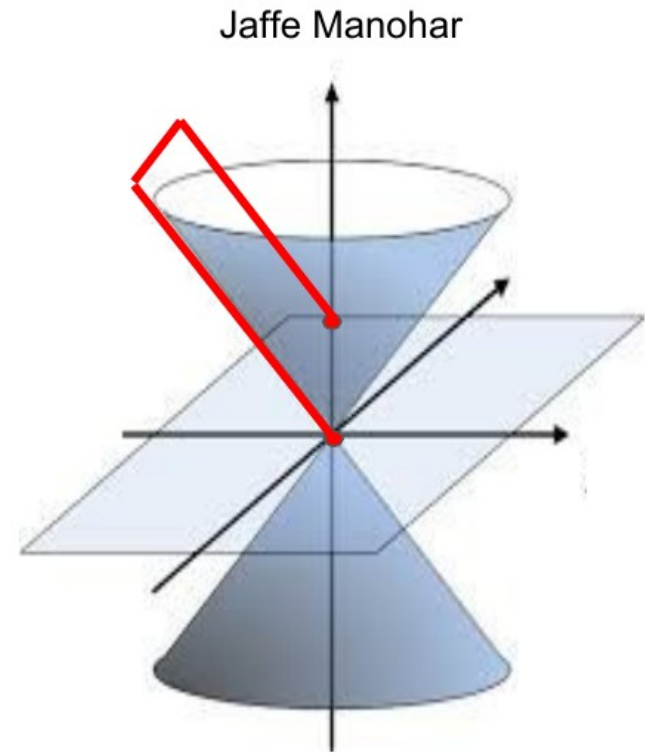


$$\frac{1}{2} = \frac{\Delta\Sigma}{2} + \mathcal{L}_q + \Delta G + \mathcal{L}_g$$

Another Look at OAM



$$L_q = \int d^3r \langle P', \Lambda' | \bar{\psi} \gamma^+ (\vec{r} \times i\vec{D}) \psi | P, \Lambda \rangle$$



$$\mathcal{L}_q = \int d^3r \langle P', \Lambda' | \bar{\psi} \gamma^+ (\vec{r} \times i\vec{D}) \psi | P, \Lambda \rangle_5$$

Another Look at OAM

How do we describe the orbital angular momentum of the partons?

$$\vec{L} = \vec{r} \times \vec{p}$$

Classically

$$L_z^q = - \left(k_T \times b_T \right)_z^q$$

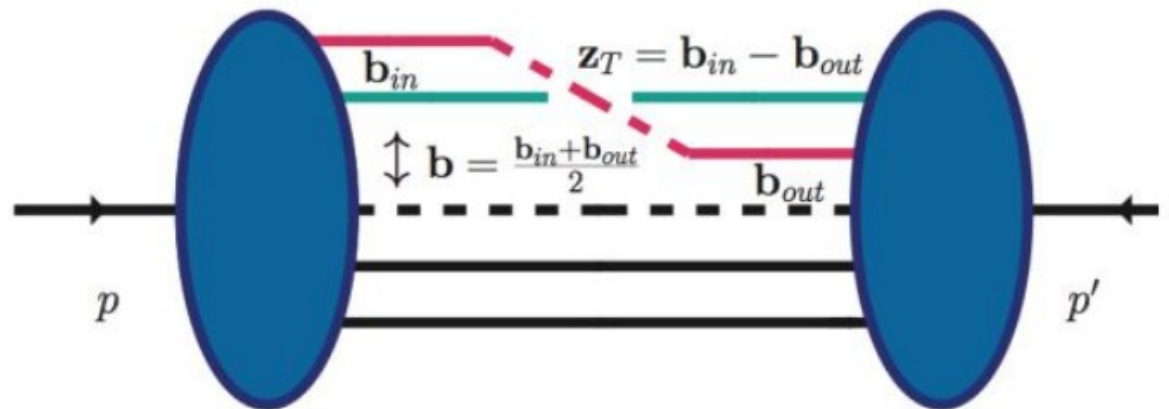
Partonic

b_T

Relative average transverse position from the center of momentum of the system

k_T

Relative average transverse momentum



Another Look at OAM

How do we describe the orbital angular momentum of the partons?

$$\vec{L} = \vec{r} \times \vec{p}$$

Classically

$$L_z^q = - \left(k_T \times b_T \right)_z^q$$

Partonic



b_T

Relative average transverse position from the center of momentum of the system

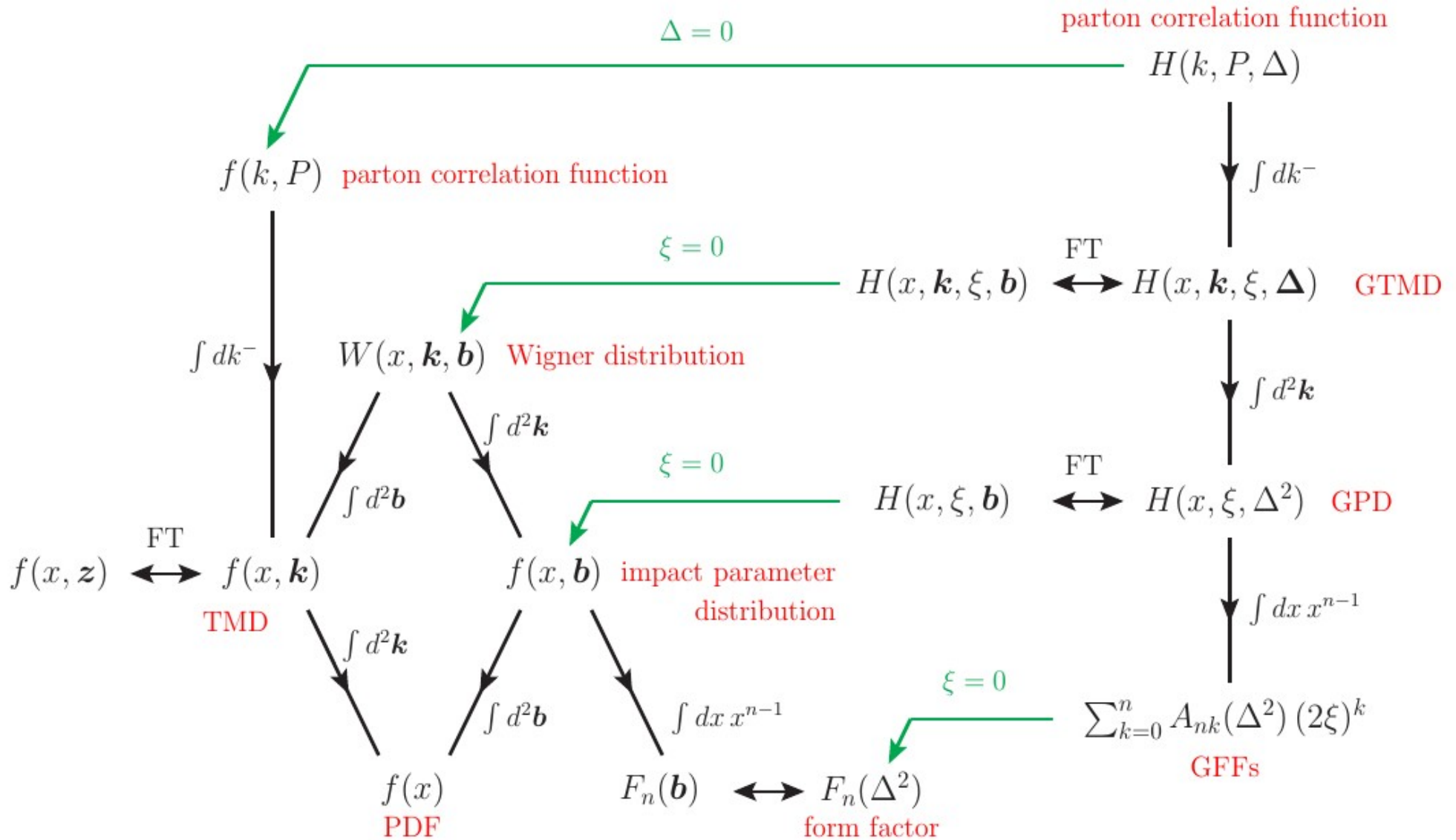
k_T

Relative average transverse momentum

$$l_z^q = \int dx d^2 k_T d^2 b_T \left(b_T \times k_T \right)_z^q \rho^{[\gamma^+]}(b_T, k_T, x)$$

$$l_z^q = - \int dx d^2 k_T \frac{k_T^2}{M^2} F_{1,4}^q$$

Hierarchy of Hadron SF



GPCF/GTMD/GPD

GPCFs

$$W_{\Lambda, \Lambda'}^\Gamma = \int \frac{d^4 z}{(2\pi)^4} e^{ik \cdot z} \left\langle P + \frac{\Delta}{2} \left| \bar{\psi}\left(-\frac{z}{2}\right) \Gamma \mathcal{U}\left(-\frac{z}{2}, \frac{z}{2}\right) \psi\left(\frac{z}{2}\right) \right| P - \frac{\Delta}{2} \right\rangle$$

$\int dk^-$

GTMDs

$$W_{\Lambda, \Lambda'}^\Gamma = \int \frac{dz^- d^2 z_\perp}{(2\pi)^3} e^{ik \cdot z} \left\langle P + \frac{\Delta}{2} \left| \bar{\psi}\left(-\frac{z}{2}\right) \Gamma \mathcal{U}\left(-\frac{z}{2}, \frac{z}{2}\right) \psi\left(\frac{z}{2}\right) \right| P - \frac{\Delta}{2} \right\rangle \Big|_{z^+ = 0}$$

$\int d^2 k_\perp$

GPDs

$$W_{\Lambda, \Lambda'}^\Gamma = \int \frac{dz^-}{2\pi} e^{izP^+ + z^-} \left\langle P + \frac{\Delta}{2} \left| \bar{\psi}\left(-\frac{z}{2}\right) \Gamma \mathcal{U}\left(-\frac{z}{2}, \frac{z}{2}\right) \psi\left(\frac{z}{2}\right) \right| P - \frac{\Delta}{2} \right\rangle$$

Sum Rules for OAM

No framework yet for GTMD observables

$$\frac{d}{dx} \int d^2 k_T \frac{k_T^2}{M^2} F_{1,4} = H + E + \tilde{E}_{2T}$$

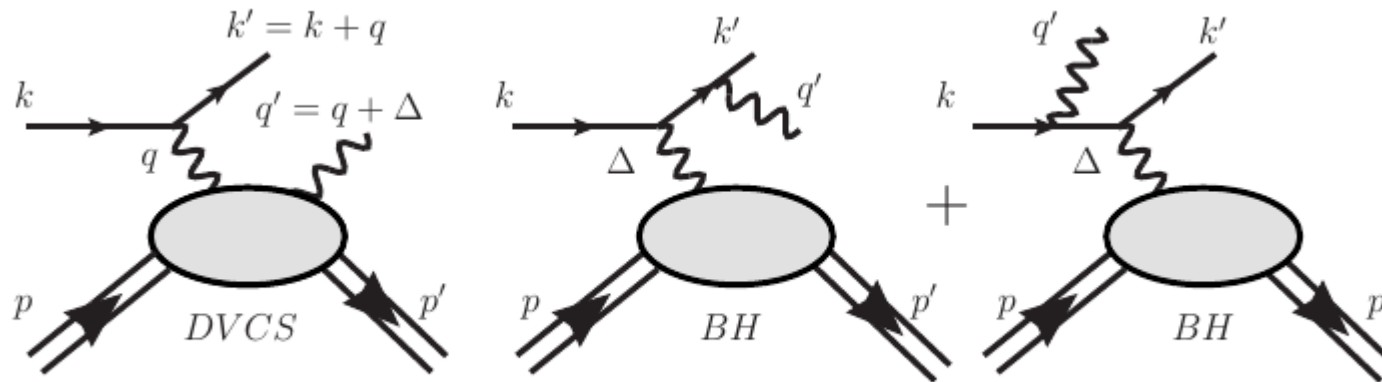
Twist-2

Twist-3



Can we disentangle the Twist-3 GPDs from data?

Exclusive Imaging

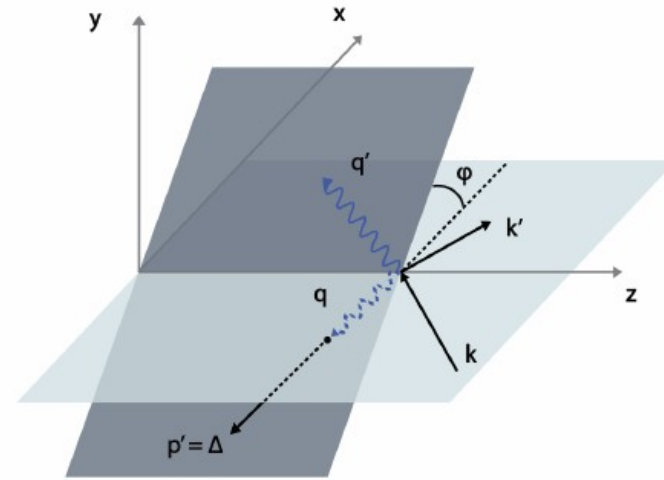
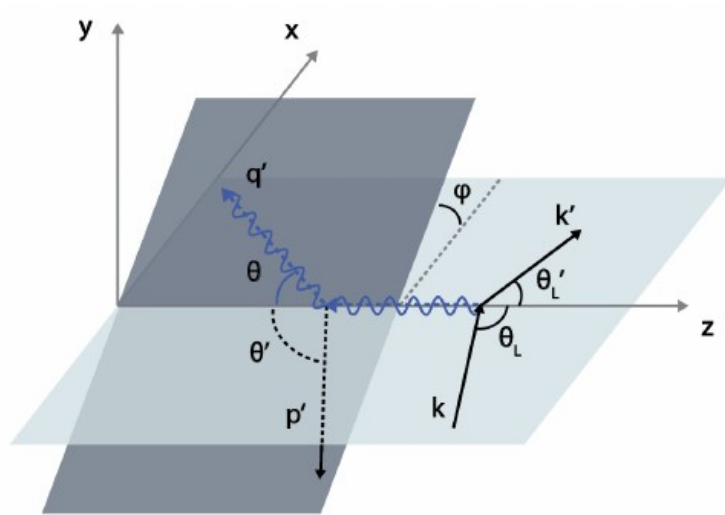


$$|T|^2 = |T_{BH} + T_{DVCS}|^2 = |T_{BH}|^2 + |T_{DVCS}|^2 + \mathcal{I}$$

$$\begin{aligned} \text{(DVCS)} \quad & \gamma^*(q) + p \rightarrow \gamma'(q') + p', \\ \text{(BH)} \quad & \gamma^*(q) + p \rightarrow p' \end{aligned}$$

$$\mathcal{I} = T_{BH}^* T_{DVCS} + T_{DVCS}^* T_{BH}.$$

DVCS + BH



$$|T|^2 = |T_{BH} + T_{DVCS}|^2 = |T_{BH}|^2 + |T_{DVCS}|^2 + \mathcal{I}$$

$$(DVCS) \quad \gamma^*(q) + p \rightarrow \gamma'(q') + p',$$

$$(BH) \quad \gamma^*(q) + p \rightarrow p'$$

$$\mathcal{I} = T_{BH}^* T_{DVCS} + T_{DVCS}^* T_{BH}.$$


Standard School

Dieter Müller


$$|\mathcal{T}_{\text{BH}}|^2 = \frac{e^6 (1 + \epsilon^2)^{-2}}{x_{\text{Bj}}^2 y^2 \Delta^2 \mathcal{P}_1(\phi) \mathcal{P}_2(\phi)} \left\{ c_0^{\text{BH}} + \sum_{n=1}^2 c_n^{\text{BH}} \cos(n\phi) \right\},$$

exactly known
(LO, QED)

$$|\mathcal{T}_{\text{DVCS}}|^2 = \frac{e^6}{y^2 Q^2} \left\{ c_0^{\text{DVCS}} + \sum_{n=1}^2 [c_n^{\text{DVCS}} \cos(n\phi) + s_n^{\text{DVCS}} \sin(n\phi)] \right\},$$

harmonics
 **1:1**
helicity ampl.

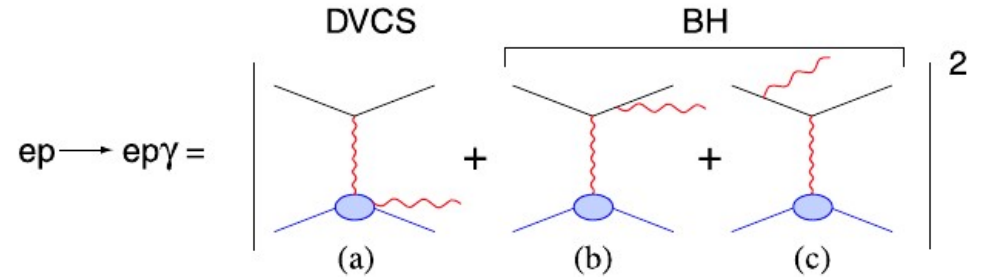
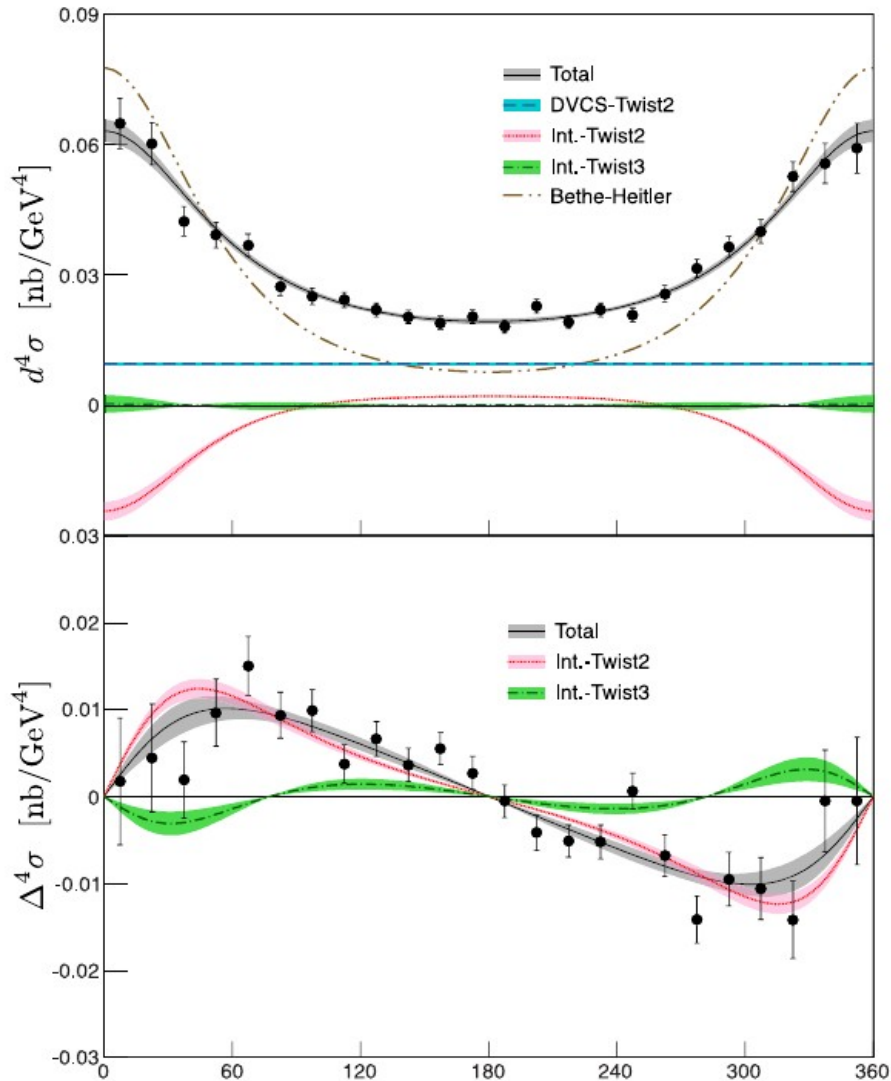
$$\mathcal{I} = \frac{\pm e^6}{x_{\text{Bj}} y^3 \Delta^2 \mathcal{P}_1(\phi) \mathcal{P}_2(\phi)} \left\{ c_0^{\mathcal{I}} + \sum_{n=1}^3 [c_n^{\mathcal{I}} \cos(n\phi) + s_n^{\mathcal{I}} \sin(n\phi)] \right\}.$$

harmonics
 **1:1**
helicity ampl.

<i>chiral even GPDs:</i>	$F = \{H, E, \tilde{H}, \tilde{E}\}$	& CFFs:	$\mathcal{F} = \{\mathcal{H}, \mathcal{E}, \tilde{\mathcal{H}}, \tilde{\mathcal{E}}\}$
<i>chiral odd GPDs:</i>	$F_T = \{H_T, E_T, \tilde{H}_T, \tilde{E}_T\}$		$\mathcal{F}_T = \{\mathcal{H}_T, \mathcal{E}_T, \tilde{\mathcal{H}}_T, \tilde{\mathcal{E}}_T\}$

DCVS Cross Section: Azimuthal Analysis

$$Q^2 = 2.36 \text{ GeV}^2, x_B = 0.37, -t = 0.32 \text{ GeV}^2$$



$$d^4\sigma = \mathcal{T}_{\text{BH}}^2 + \mathcal{T}_{\text{BH}} \text{Re}(\mathcal{T}_{\text{DVCS}}) + \mathcal{T}_{\text{DVCS}}^2$$

$$\text{Re}(\mathcal{T}_{\text{DVCS}}) \sim c_0^{\mathcal{I}} + c_1^{\mathcal{I}} \cos \phi + c_2^{\mathcal{I}} \cos 2\phi$$

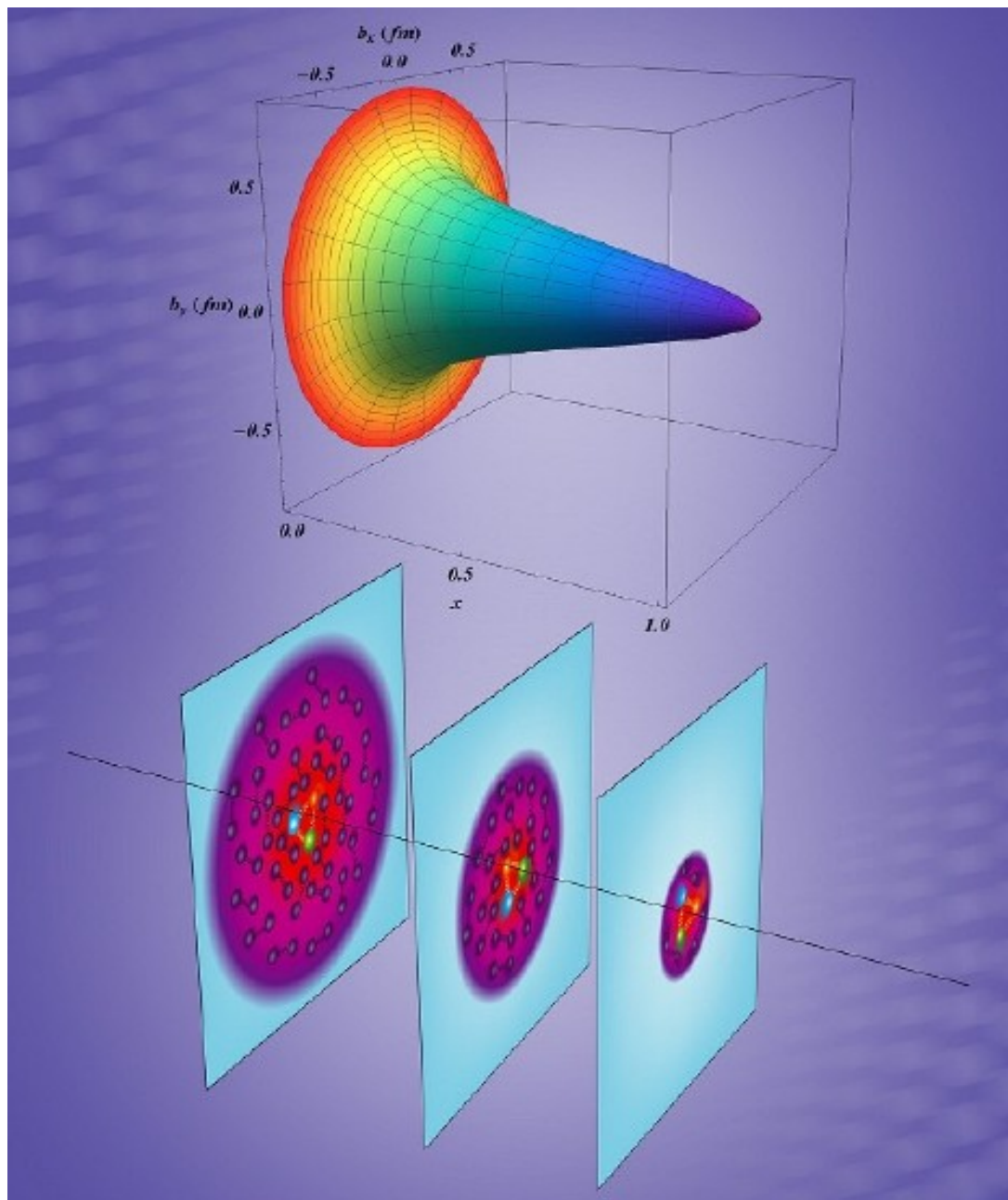
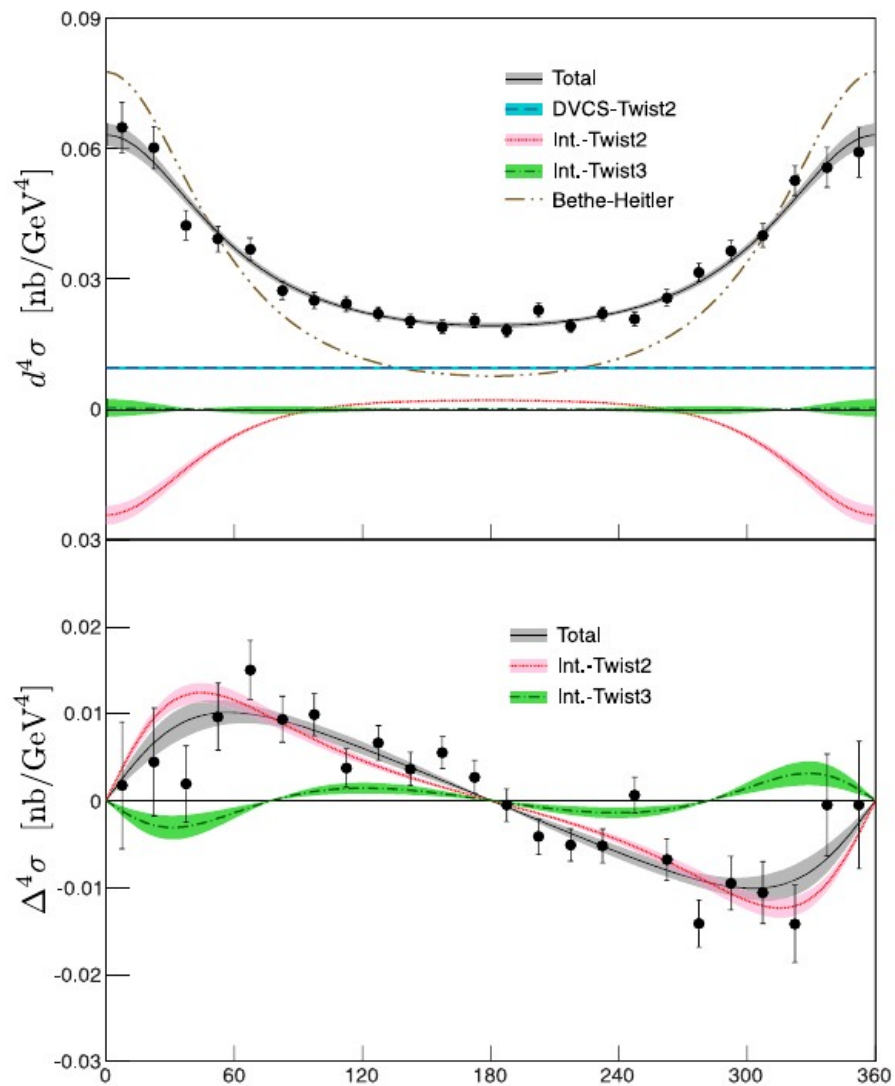
$$\mathcal{T}_{\text{DVCS}}^2 \sim c_0^{\text{DVCS}} + c_1^{\text{DVCS}} \cos \phi$$

$$\Delta^4\sigma = \frac{d^4\vec{\sigma} - d^4\overleftarrow{\sigma}}{2} = \text{Im}(\mathcal{T}_{\text{DVCS}})$$

$$\text{Im}(\mathcal{T}_{\text{DVCS}}) \sim s_1^{\mathcal{I}} \sin \phi + s_2^{\mathcal{I}} \sin 2\phi$$






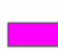
DCVS Cross Section: Azimuthal Analysis

$$Q^2 = 2.36 \text{ GeV}^2, x_B = 0.37, -t = 0.32 \text{ GeV}^2$$



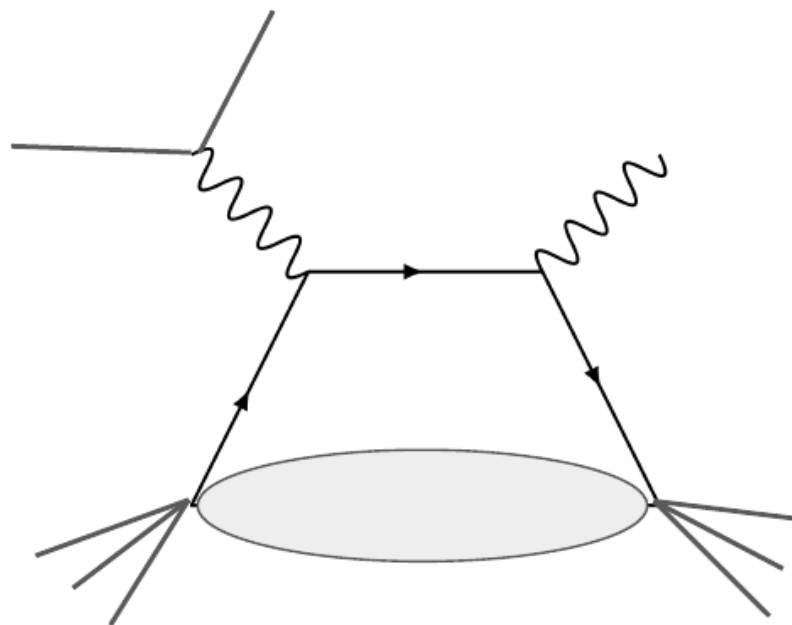
DVCS Cross Section

$$\frac{d^5\sigma_{DVCS}}{dx_{Bj}dQ^2d|t|d\phi d\phi_S} = \Gamma |T_{DVCS}|^2$$

Unpolarized		$= \frac{\Gamma}{Q^2(1-\epsilon)} \left\{ F_{UU,T} + \epsilon F_{UU,L} + \epsilon \cos 2\phi F_{UU}^{\cos 2\phi} + \sqrt{\epsilon(\epsilon+1)} \cos \phi F_{UU}^{\cos \phi} \right.$
LU polarized		$+ (2h) \sqrt{2\epsilon(1-\epsilon)} \sin \phi F_{LU}^{\sin \phi}$
UL polarized		$+ (2\Lambda) \left[\sqrt{\epsilon(\epsilon+1)} \sin \phi F_{UL}^{\sin \phi} + \epsilon \sin 2\phi F_{UL}^{\sin 2\phi} \right.$
LL polarized		$+ (2h) \left(\sqrt{1-\epsilon^2} F_{LL} + 2\sqrt{\epsilon(1-\epsilon)} \cos \phi F_{LL}^{\cos \phi} \right) \left. \right]$
UT polarized		$+ (2\Lambda_T) \left[\sin(\phi - \phi_S) \left(F_{UT,T}^{\sin(\phi-\phi_S)} + \epsilon F_{UT,L}^{\sin(\phi-\phi_S)} \right) \right.$
		$+ \epsilon \sin(\phi + \phi_S) F_{UT}^{\sin(\phi+\phi_S)} + \epsilon \sin(3\phi - \phi_S) F_{UT}^{\sin(3\phi-\phi_S)}$
		$+ \sqrt{2\epsilon(1+\epsilon)} \left(\sin \phi_S F_{UT}^{\sin \phi_S} + \sin(2\phi - \phi_S) F_{UT}^{\sin(2\phi-\phi_S)} \right) \left. \right]$
LT polarized		$+ (2h)(2\Lambda_T) \left[\sqrt{1-\epsilon^2} \cos(\phi - \phi_S) F_{LT}^{\cos(\phi-\phi_S)} + \sqrt{2\epsilon(1-\epsilon)} \cos \phi_S F_{LT}^{\cos \phi_S} \right.$
		$+ \left. \left. \sqrt{2\epsilon(1-\epsilon)} \cos(2\phi - \phi_S) F_{LT}^{\cos(2\phi-\phi_S)} \right] \right\}$

- Twist 2: $F_{UU,T}, F_{LL}, F_{UT,T}^{\sin(\phi-\phi_S)}, F_{LT}^{\cos(\phi-\phi_S)}$
- Twist 3: $F_{UU}^{\cos \phi}, F_{UL}^{\sin \phi}, F_{LU}^{\sin \phi}, F_{LL}^{\cos \phi}, F_{UT}^{\sin \phi_S}, F_{UT}^{\sin(2\phi-\phi_S)}, F_{LT}^{\cos \phi_S}, F_{LT}^{\cos(2\phi-\phi_S)}$
- Twist 4: $F_{UU,L}, F_{UT,L}^{\sin(\phi-\phi_S)}$

DVCS



— Twist - 2
— Twist - 3

$$W^{\mu\nu} \propto \gamma^\mu \gamma^+ \gamma^\nu = \begin{bmatrix} \gamma^- & \gamma^1 - i\gamma^2\gamma_5 & \gamma^2 + i\gamma^1\gamma_5 & i\gamma^- \gamma_5 \\ \boxed{\gamma^1 + i\gamma^2\gamma_5} & \boxed{\gamma^+} & \boxed{i\gamma^+ \gamma_5} & \boxed{-\gamma^1 - i\gamma^2\gamma_5} \\ \boxed{\gamma^2 - i\gamma^1\gamma_5} & \boxed{-i\gamma^+ \gamma_5} & \boxed{\gamma^+} & \boxed{-\gamma^2 + i\gamma^1\gamma_5} \\ -i\gamma^- \gamma_5 & -\gamma^1 + i\gamma^2\gamma_5 & -\gamma^2 - i\gamma^1\gamma_5 & \gamma^- \end{bmatrix}$$

Twist-2 Observables

$$F_{UU,T} = 4 \left[(1 - \xi^2) \left(|\mathcal{H}|^2 + |\tilde{\mathcal{H}}|^2 \right) + \frac{t_o - t}{2M^2} \left(|\mathcal{E}|^2 + \xi^2 |\tilde{\mathcal{E}}|^2 \right) - \frac{2\xi^2}{1 - \xi^2} \Re \left(\mathcal{H}\mathcal{E} + \tilde{\mathcal{H}}\tilde{\mathcal{E}} \right) \right]$$

$$F_{LL} = 2 \left[2(1 - \xi^2) |\mathcal{H}\tilde{\mathcal{H}}| + 4\xi \frac{t_o - t}{2M^2} |\mathcal{E}\tilde{\mathcal{E}}| + \frac{2\xi^2}{1 - \xi^2} \Re \left(\mathcal{H}\tilde{\mathcal{E}} + \tilde{\mathcal{H}}\mathcal{E} \right) \right]$$

$$F_{UT,T}^{\sin(\phi - \phi_S)} = -\frac{\sqrt{t_o - t}}{2M} \left[\Re \left(\tilde{\mathcal{H}} - \frac{\xi^2}{1 - \xi^2} \tilde{\mathcal{E}} \right) \Im m \mathcal{E} - \xi \Re \left(\mathcal{H} - \frac{\xi^2}{1 - \xi^2} \mathcal{E} \right) \Im m \tilde{\mathcal{E}} \right. \\ \left. - \Im m \left(\tilde{\mathcal{H}} - \frac{\xi^2}{1 - \xi^2} \tilde{\mathcal{E}} \right) \Re \mathcal{E} + \xi \Im m \left(\mathcal{H} - \frac{\xi^2}{1 - \xi^2} \mathcal{E} \right) \Re \tilde{\mathcal{E}} \right]$$

Twist-3 Observables

$$\begin{aligned}
 F_{UU}^{\cos\phi} = & -2(1-\xi^2)\Re\left[\left(2\tilde{\mathcal{H}}_{2T} + \mathcal{E}_{2T} + 2\tilde{\mathcal{H}}'_{2T} + \mathcal{E}'_{2T}\right)\left(\mathcal{H} - \frac{\xi^2}{1-\xi^2}\mathcal{E}\right)\right. \\
 & - 2\xi\left(\tilde{\mathcal{E}}_{2T} + \tilde{\mathcal{E}}'_{2T}\right)\left(\tilde{\mathcal{H}} - \frac{\xi^2}{1-\xi^2}\tilde{\mathcal{E}}\right) + \frac{t_0-t}{16M^2}\left(\tilde{\mathcal{H}}_{2T} + \tilde{\mathcal{H}}'_{2T}\right)\left(\mathcal{E} + \xi\tilde{\mathcal{E}}\right) \\
 & + \left(\mathcal{H}_{2T} + \mathcal{H}'_{2T} + \frac{t_0-t}{4M^2}\left(\tilde{\mathcal{H}}_{2T} + \tilde{\mathcal{H}}'_{2T}\right) + \frac{\xi}{1-\xi^2}\left(\tilde{\mathcal{E}}_{2T} + \tilde{\mathcal{E}}'_{2T}\right)\right) \\
 & \left. - \frac{\xi^2}{1-\xi^2}\left(\mathcal{E}_{2T} + \mathcal{E}'_{2T}\right)\right]\left(\mathcal{E} - \xi\tilde{\mathcal{E}}\right)
 \end{aligned}$$

What are these linear combinations of GPDs?

$$\begin{aligned}
 F_{LU}^{\sin\phi} = & -2(1-\xi^2)\Im\left[\left(2\tilde{\mathcal{H}}_{2T} + \mathcal{E}_{2T} + 2\tilde{\mathcal{H}}'_{2T} + \mathcal{E}'_{2T}\right)\left(\mathcal{H} - \frac{\xi^2}{1-\xi^2}\mathcal{E}\right)\right. \\
 & - 2\xi\left(\tilde{\mathcal{E}}_{2T} + \tilde{\mathcal{E}}'_{2T}\right)\left(\tilde{\mathcal{H}} - \frac{\xi^2}{1-\xi^2}\tilde{\mathcal{E}}\right) + \frac{t_0-t}{16M^2}\left(\tilde{\mathcal{H}}_{2T} + \tilde{\mathcal{H}}'_{2T}\right)\left(\mathcal{E} + \xi\tilde{\mathcal{E}}\right) \\
 & + \left[\left(\mathcal{H}_{2T} + \mathcal{H}'_{2T} + \frac{t_0-t}{4M^2}\left(\tilde{\mathcal{H}}_{2T} + \tilde{\mathcal{H}}'_{2T}\right) + \frac{\xi}{1-\xi^2}\left(\tilde{\mathcal{E}}_{2T} + \tilde{\mathcal{E}}'_{2T}\right)\right) \right. \\
 & \left. - \frac{\xi^2}{1-\xi^2}\left(\mathcal{E}_{2T} + \mathcal{E}'_{2T}\right)\right]\left(\mathcal{E} - \xi\tilde{\mathcal{E}}\right)
 \end{aligned}$$

Get access to 8 Form Factors from DVCS alone.

Observables

GPD	Twist	$P_q P_p$	TMD
$\mathbf{H} + \frac{\xi^2}{1-\xi} \mathbf{E}$	2	UU	f_1
$\tilde{\mathbf{H}} + \frac{\xi^2}{1-\xi} \tilde{\mathbf{E}}$	2	LL	g_1
\mathbf{E}	2	UT	$f_{1T}^{\perp(*)}$
$\tilde{\mathbf{E}}$	2	LT	g_{1T}
$\mathbf{H} + \mathbf{E}$	2	-	-

GPD	Twist	$P_q P_p$	TMD
$2\tilde{\mathbf{H}}_{2T} + \mathbf{E}_{2T} - \xi \tilde{\mathbf{E}}_{2T}$	3	UU	f^{\perp}
$2\tilde{\mathbf{H}}'_{2T} + \mathbf{E}'_{2T} - \xi \tilde{\mathbf{E}}'_{2T}$	3	LL	g_L^{\perp}
$\mathbf{H}_{2T} + \frac{t_o - t}{4M^2} \tilde{\mathbf{H}}_{2T}$	3	UT	$f_T^{(*)}, f_T^{\perp(*)}$
$\mathbf{H}'_{2T} + \frac{t_o - t}{4M^2} \tilde{\mathbf{H}}'_{2T}$	3	LT	g'_T, g_T^{\perp}
$\tilde{\mathbf{E}}_{2T} - \xi \mathbf{E}_{2T}$	3	UL	$f_L^{\perp(*)}$
$\tilde{\mathbf{E}}'_{2T} - \xi \mathbf{E}'_{2T}$	3	LU	$g^{\perp(*)}$
$\tilde{\mathbf{H}}_{2T}$	3	UT _x	$f_T^{\perp(*)}$
$\tilde{\mathbf{H}}'_{2T}$	3	LT _x	g_T^{\perp}

Additional Information

$$\text{OAM} \quad \boxed{\frac{1}{\sqrt{1-\xi^2}} \frac{\Delta_{\perp}}{P^+} \left(\tilde{E}_{2T} - \xi E_{2T} \right) e^{i\phi}} = W_{++}^{\gamma^1} + iW_{++}^{\gamma^2} - W_{--}^{\gamma^1} - iW_{--}^{\gamma^2}$$

$$\frac{1}{\sqrt{1-\xi^2}} \frac{\Delta_{\perp}}{P^+} \left(E_{2T} - \xi \tilde{E}_{2T} + 2\tilde{H}_{2T} \right) e^{i\phi} = W_{++}^{\gamma^1} + iW_{++}^{\gamma^2} + W_{--}^{\gamma^1} + iW_{--}^{\gamma^2}$$

$$\frac{1}{\sqrt{1-\xi^2}} \frac{\Delta_{\perp}^2}{MP^+} 2\tilde{H}_{2T} = \left(W_{-+}^{\gamma^1} - iW_{-+}^{\gamma^2} \right) e^{2i\phi} - \left(W_{+-}^{\gamma^1} + iW_{+-}^{\gamma^2} \right) e^{-2i\phi}$$

$$\frac{1}{\sqrt{1-\xi^2}} \frac{4M}{P^+} \left(\tilde{E}_{2T} - \xi E_{2T} - (1-\xi^2)H_{2T} - \frac{\Delta_{\perp}^2}{4M^2} \tilde{H}_{2T} \right) = W_{+-}^{\gamma^1} - iW_{+-}^{\gamma^2} - W_{-+}^{\gamma^1} - iW_{-+}^{\gamma^2}$$

Additional Information

$$\frac{1}{\sqrt{1-\xi^2}} \frac{\Delta_{\perp}}{P^+} \left(\tilde{E}'_{2T} - \xi E'_{2T} \right) e^{i\phi} = W_{++}^{\gamma^1 \gamma^5} + iW_{++}^{\gamma^2 \gamma^5} - W_{--}^{\gamma^1 \gamma^5} - iW_{--}^{\gamma^2 \gamma^5}$$

Spin-
Orbit

$$\left[\frac{1}{\sqrt{1-\xi^2}} \frac{\Delta_{\perp}}{P^+} \left(E'_{2T} - \xi \tilde{E}'_{2T} + 2\tilde{H}'_{2T} \right) e^{i\phi} \right] = W_{++}^{\gamma^1 \gamma^5} + iW_{++}^{\gamma^2 \gamma^5} + W_{--}^{\gamma^1 \gamma^5} + iW_{--}^{\gamma^2 \gamma^5}$$

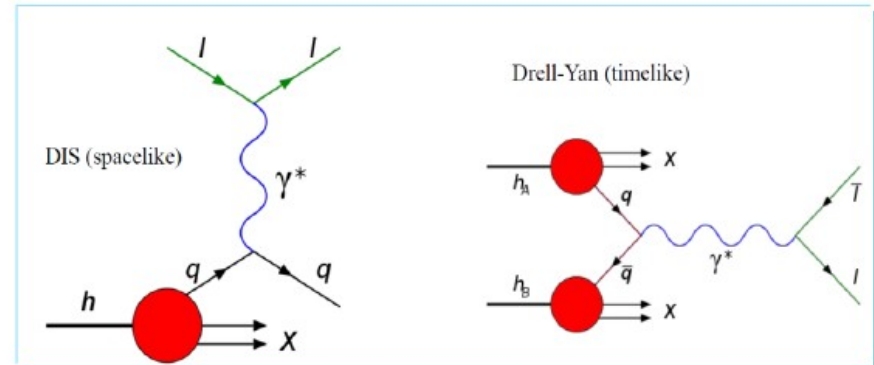
$$-\frac{1}{\sqrt{1-\xi^2}} \frac{\Delta_{\perp}^2}{MP^+} 2\tilde{H}'_{2T} = \left(W_{+-}^{\gamma^1 \gamma^5} + iW_{+-}^{\gamma^2 \gamma^5} \right) e^{-2i\phi} + \left(W_{-+}^{\gamma^1 \gamma^5} - iW_{-+}^{\gamma^2 \gamma^5} \right) e^{2i\phi}$$

$$\frac{1}{\sqrt{1-\xi^2}} \frac{4M}{P^+} \left(\tilde{E}'_{2T} - \xi E'_{2T} + (1-\xi^2)H'_{2T} + \frac{\Delta_T^2}{4M^2} \tilde{H}'_{2T} \right) = W_{+-}^{\gamma^1 \gamma^5} - iW_{+-}^{\gamma^2 \gamma^5} + W_{-+}^{\gamma^1 \gamma^5} + iW_{-+}^{\gamma^2 \gamma^5}$$

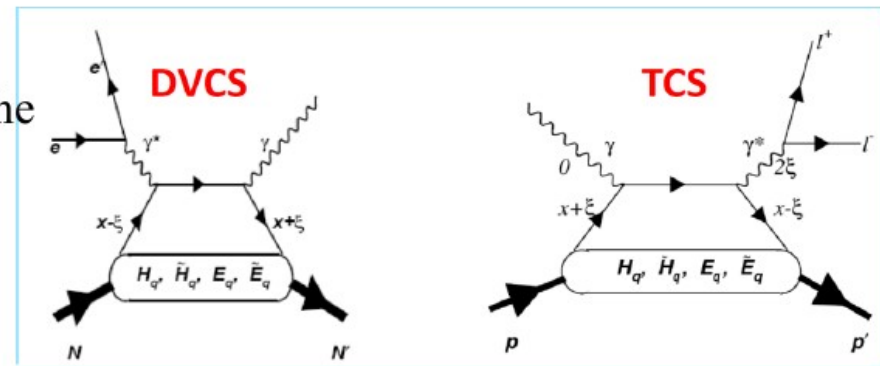
Timelike-Spacelike

- Spacelike DIS and timelike Drell-Yan processes both factorize into partonic cross section and a Parton Distribution Function (PDF)

- Measurement of both demonstrated the universality of PDFs

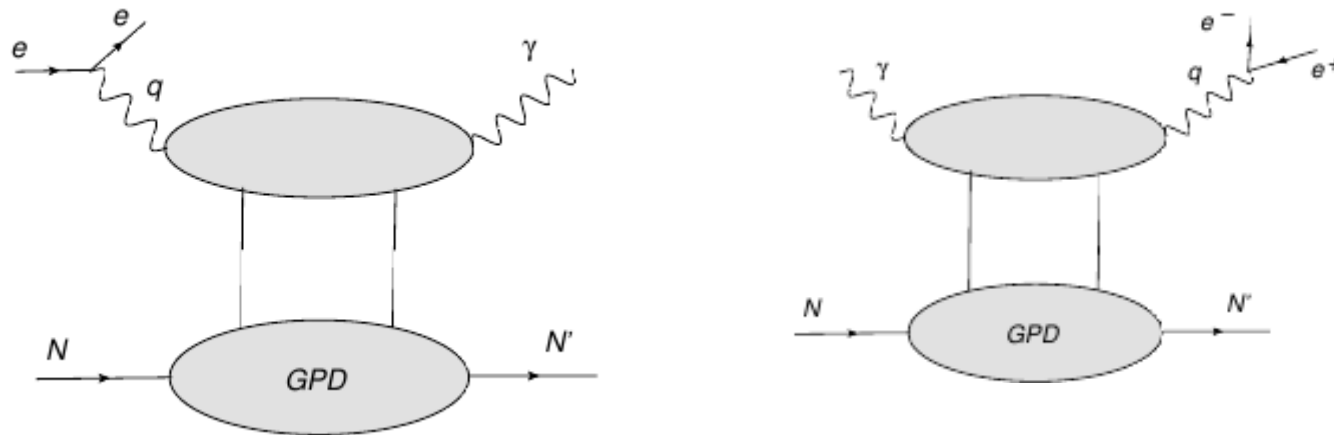


- In Deeply Virtual Compton Scattering (DVCS) there is a similar factorization at the amplitude level into a perturbative coefficient function and a Generalized Parton Distribution (GPD)



In TCS the real part of the scattering amplitude can be accessed through the azimuthal angular asymmetry of lepton pair (unpolarized beam and target) or through the spin asymmetries (polarized beam and/or polarized target).

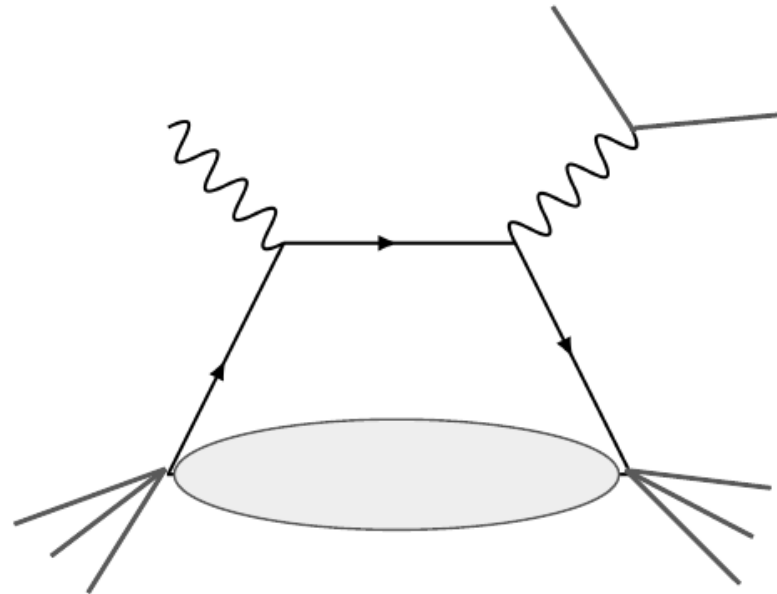
Timelike Compton Scattering



$$\gamma(q)N(p) \rightarrow \gamma^*(q')N(p') \rightarrow l^-(k)l^+(k')N(p')$$

The Time Process

TCS



$$e^{i\phi} \rightarrow e^{-i\phi}$$

— Twist - 2
— Twist - 3

$$W^{\mu\nu} \propto \gamma^\mu \gamma^+ \gamma^\nu = \begin{bmatrix} \gamma^- & \gamma^1 - i\gamma^2\gamma_5 & \gamma^2 + i\gamma^1\gamma_5 & i\gamma^- \gamma_5 \\ \gamma^1 + i\gamma^2\gamma_5 & \gamma^+ & i\gamma^+ \gamma_5 & -\gamma^1 - i\gamma^2\gamma_5 \\ \gamma^2 - i\gamma^1\gamma_5 & -i\gamma^+ \gamma_5 & \gamma^+ & -\gamma^2 + i\gamma^1\gamma_5 \\ -i\gamma^- \gamma_5 & -\gamma^1 + i\gamma^2\gamma_5 & -\gamma^2 - i\gamma^1\gamma_5 & \gamma^- \end{bmatrix}$$

Combining Information

TCS

$$\begin{aligned}
 F_{UU}^{\cos\phi} = & -2(1-\xi^2)\Re\left[\left(2\tilde{\mathcal{H}}_{2T} + \mathcal{E}_{2T} - 2\tilde{\mathcal{H}}'_{2T} - \mathcal{E}'_{2T}\right)\left(\mathcal{H} - \frac{\xi^2}{1-\xi^2}\mathcal{E}\right)\right. \\
 & \left. - 2\xi\left(\tilde{\mathcal{E}}_{2T} - \tilde{\mathcal{E}}'_{2T}\right)\left(\tilde{\mathcal{H}} - \frac{\xi^2}{1-\xi^2}\tilde{\mathcal{E}}\right) + \frac{t_0-t}{16M^2}\left(\tilde{\mathcal{H}}_{2T} - \tilde{\mathcal{H}}'_{2T}\right)\left(\mathcal{E} + \xi\tilde{\mathcal{E}}\right)\right. \\
 & \left. + \left(\mathcal{H}_{2T} - \mathcal{H}'_{2T} + \frac{t_0-t}{4M^2}\left(\tilde{\mathcal{H}}_{2T} - \tilde{\mathcal{H}}'_{2T}\right) + \frac{\xi}{1-\xi^2}\left(\tilde{\mathcal{E}}_{2T} - \tilde{\mathcal{E}}'_{2T}\right)\right.\right. \\
 & \left. \left. - \frac{\xi^2}{1-\xi^2}\left(\mathcal{E}_{2T} - \mathcal{E}'_{2T}\right)\right)\left(\mathcal{E} - \xi\tilde{\mathcal{E}}\right)\right]
 \end{aligned}$$

DVCS

$$\begin{aligned}
 F_{UU}^{\cos\phi} = & -2(1-\xi^2)\Re\left[\left(2\tilde{\mathcal{H}}_{2T} + \mathcal{E}_{2T} + 2\tilde{\mathcal{H}}'_{2T} + \mathcal{E}'_{2T}\right)\left(\mathcal{H} - \frac{\xi^2}{1-\xi^2}\mathcal{E}\right)\right. \\
 & \left. - 2\xi\left(\tilde{\mathcal{E}}_{2T} + \tilde{\mathcal{E}}'_{2T}\right)\left(\tilde{\mathcal{H}} - \frac{\xi^2}{1-\xi^2}\tilde{\mathcal{E}}\right) + \frac{t_0-t}{16M^2}\left(\tilde{\mathcal{H}}_{2T} + \tilde{\mathcal{H}}'_{2T}\right)\left(\mathcal{E} + \xi\tilde{\mathcal{E}}\right)\right. \\
 & \left. + \left(\mathcal{H}_{2T} + \mathcal{H}'_{2T} + \frac{t_0-t}{4M^2}\left(\tilde{\mathcal{H}}_{2T} + \tilde{\mathcal{H}}'_{2T}\right) + \frac{\xi}{1-\xi^2}\left(\tilde{\mathcal{E}}_{2T} + \tilde{\mathcal{E}}'_{2T}\right)\right.\right. \\
 & \left. \left. - \frac{\xi^2}{1-\xi^2}\left(\mathcal{E}_{2T} + \mathcal{E}'_{2T}\right)\right)\left(\mathcal{E} - \xi\tilde{\mathcal{E}}\right)\right]
 \end{aligned}$$

$$-2\xi\tilde{\mathcal{E}}_{2T}\tilde{\mathcal{H}}$$

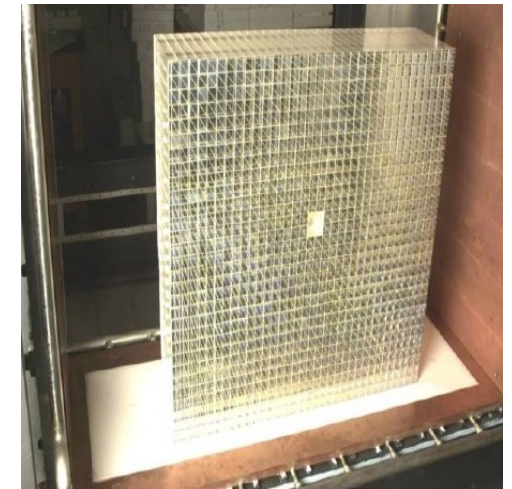
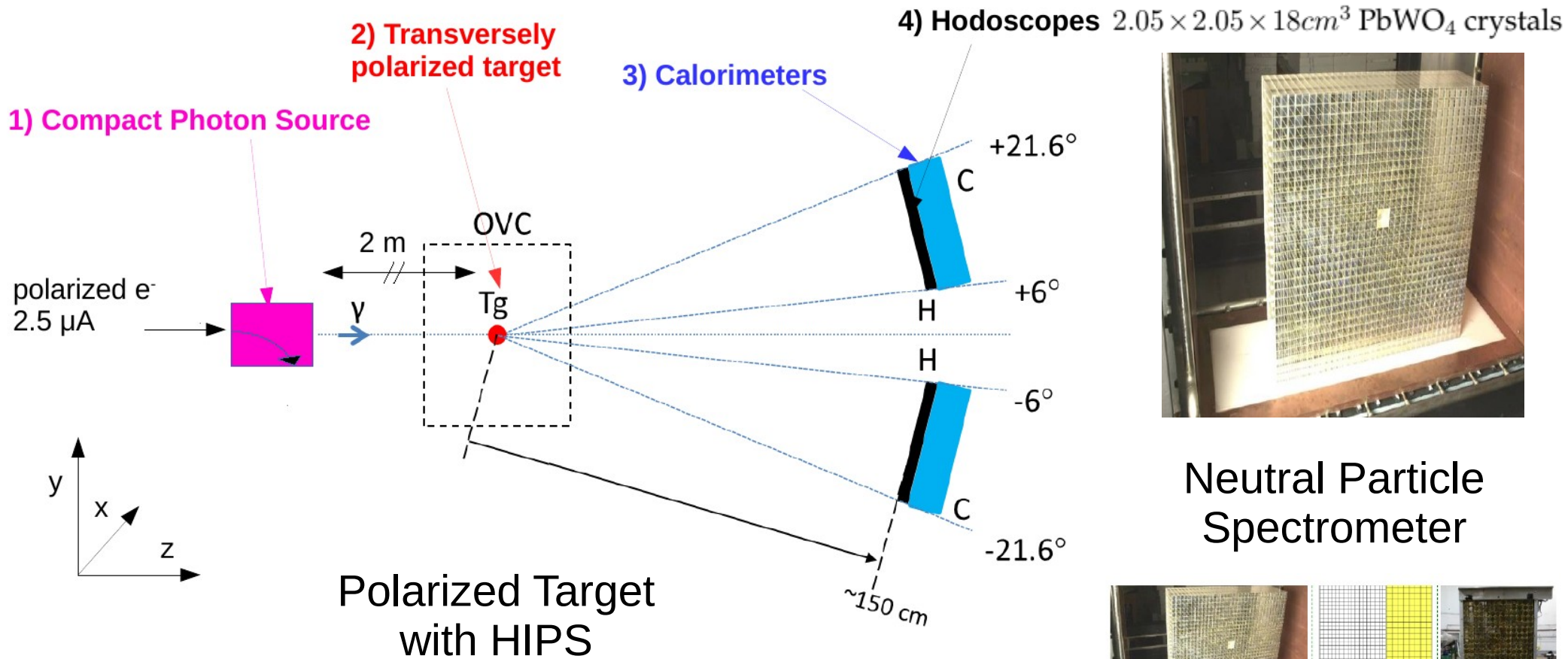
TCS with HIPS

- Jlab PAC-46: TCS off TPP → E12-18-005

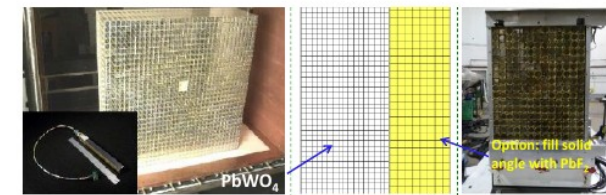
M. Boer, V. Tadevosyan, DK

- HIPS/CPS: [arxiv:1704.00816.pdf](https://arxiv.org/abs/1704.00816) B. Wojtsekhowski, D. Day, DK
- NPS: [arxiv:1704.00816.pdf](https://arxiv.org/abs/1704.00816), J. Phys. C.S.587012048, [arXiv:0609201](https://arxiv.org/abs/0609201) T. Horn, R. Ent, NPS Collaboration
- Target/CPS: NIM In Progress DK

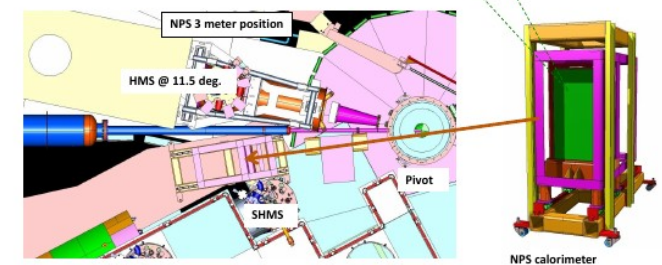
Jlab Experimental Setup



Neutral Particle Spectrometer

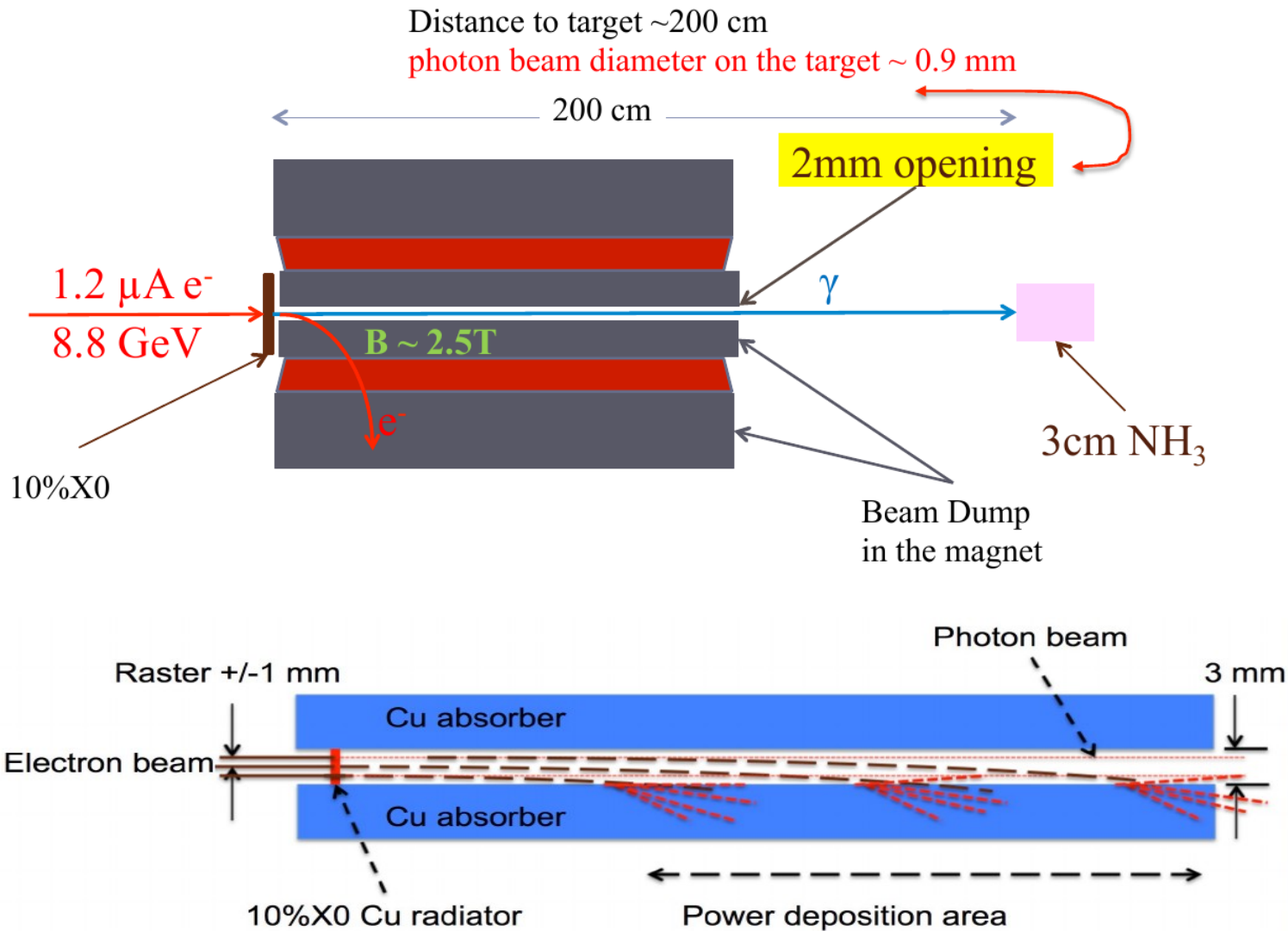


Side view of the TCS experimental setup. Shown are photon beam (γ), transversely polarized target (Tg) in the scattering chamber (OVC), and pairs of hodoscope (H) and calorimeter (C) counters for detection of the recoil proton and the lepton pair.

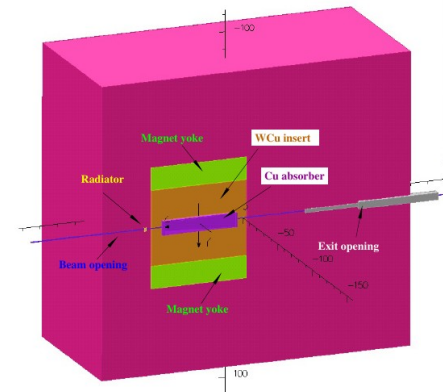
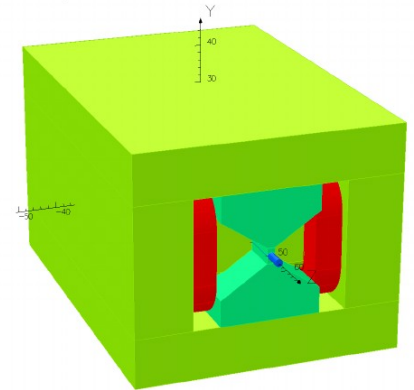


Compact Photon Source

B. Wojtsekhowski, D. Day, DK



Magnet design



High Intensity Photon Targets

- Depolarization due to radiation damage

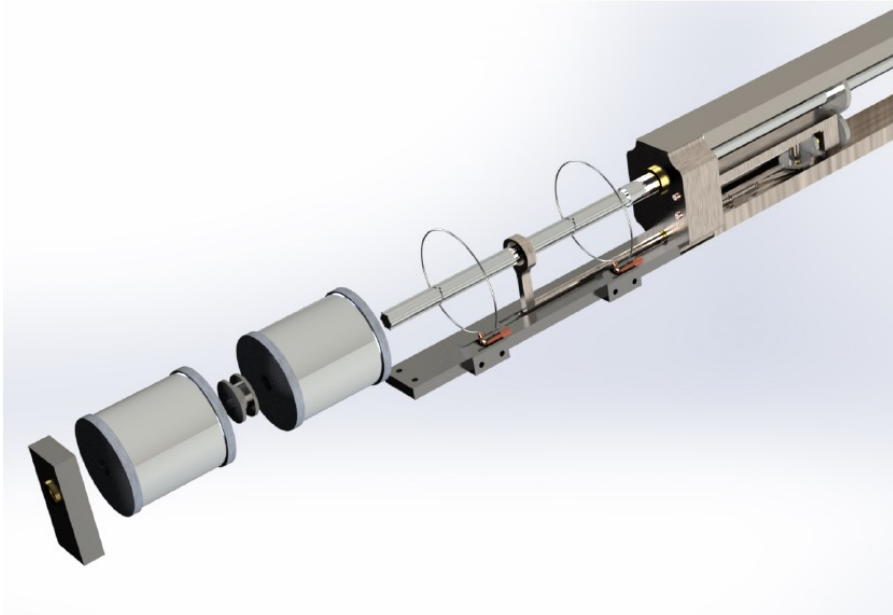
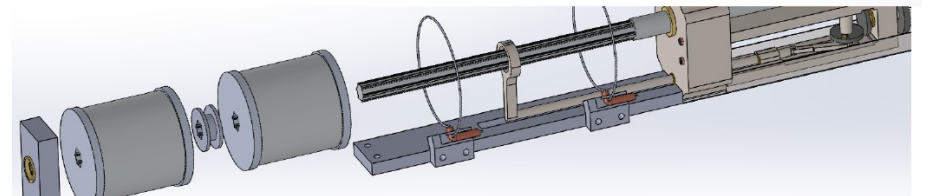
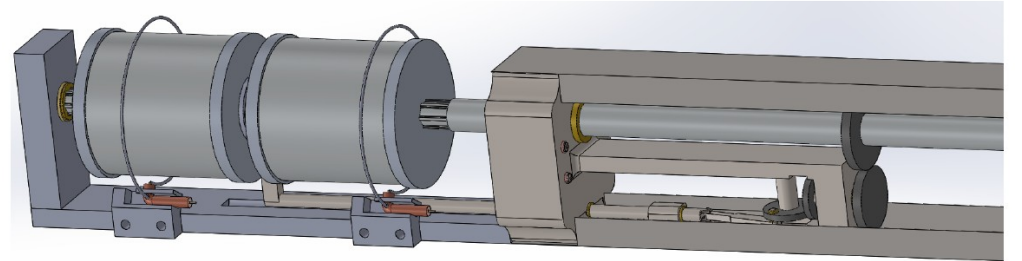
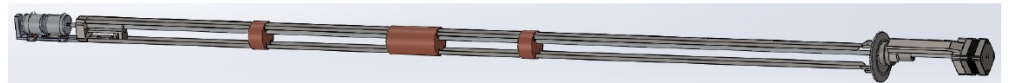
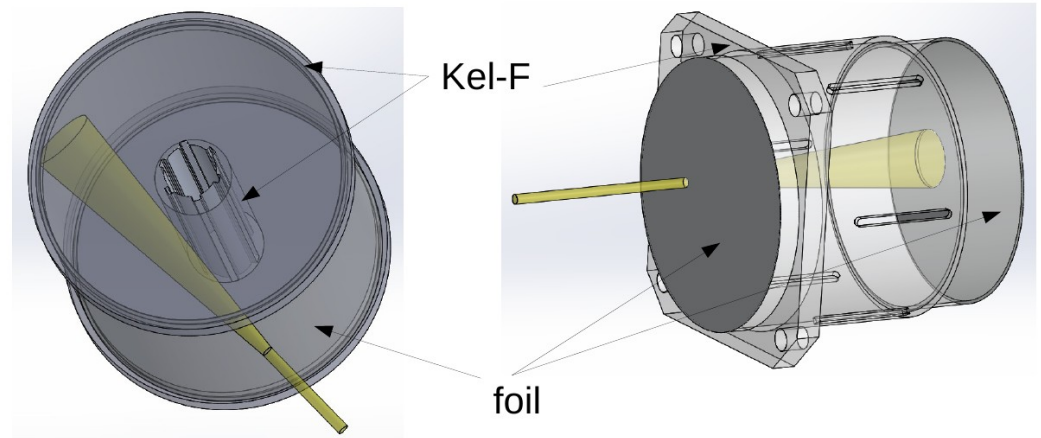
- Photons at the several GeV scale can easily break up NH₃
- Especially with high energy (IPs) we get significant production of NH₂, Atomic H, Atomic N, and recombination to hydrazine and others
- This radiation damage causes either different polarization mechanisms and/or depleted DNP
- The production of these free radicals is the leading cause of target maintenance and overhead time required to anneal and replace target material
- EGS and Geant indicate we will get some of these processes with a high energy photon but the primary production of centers is still NH₂, Atomic H from the IPs created by the photon source
- Secondary scattering of ionizing radiation inside the target using 10^{11} gamma/sec with RMS~1 mm leads to 20 nA of e⁺/e⁻ in an area of 4.5 mm²
- If this dose can be spread out over the surface of the target (570 mm²) we start to approach the radiation damage seen in CLAS6 type running

- Depolarization due to localized beam heating

- Local hot-spots caused by interfacial thermal heating can create loss of polarization at the beam location in the target
- Additional heating issue arise from thermal conductivity of the material and the Kapitza resistance
- All of this is easily handled by keeping the beam to target position moving (fix only a couple of seconds)

CPS Polarized Target System

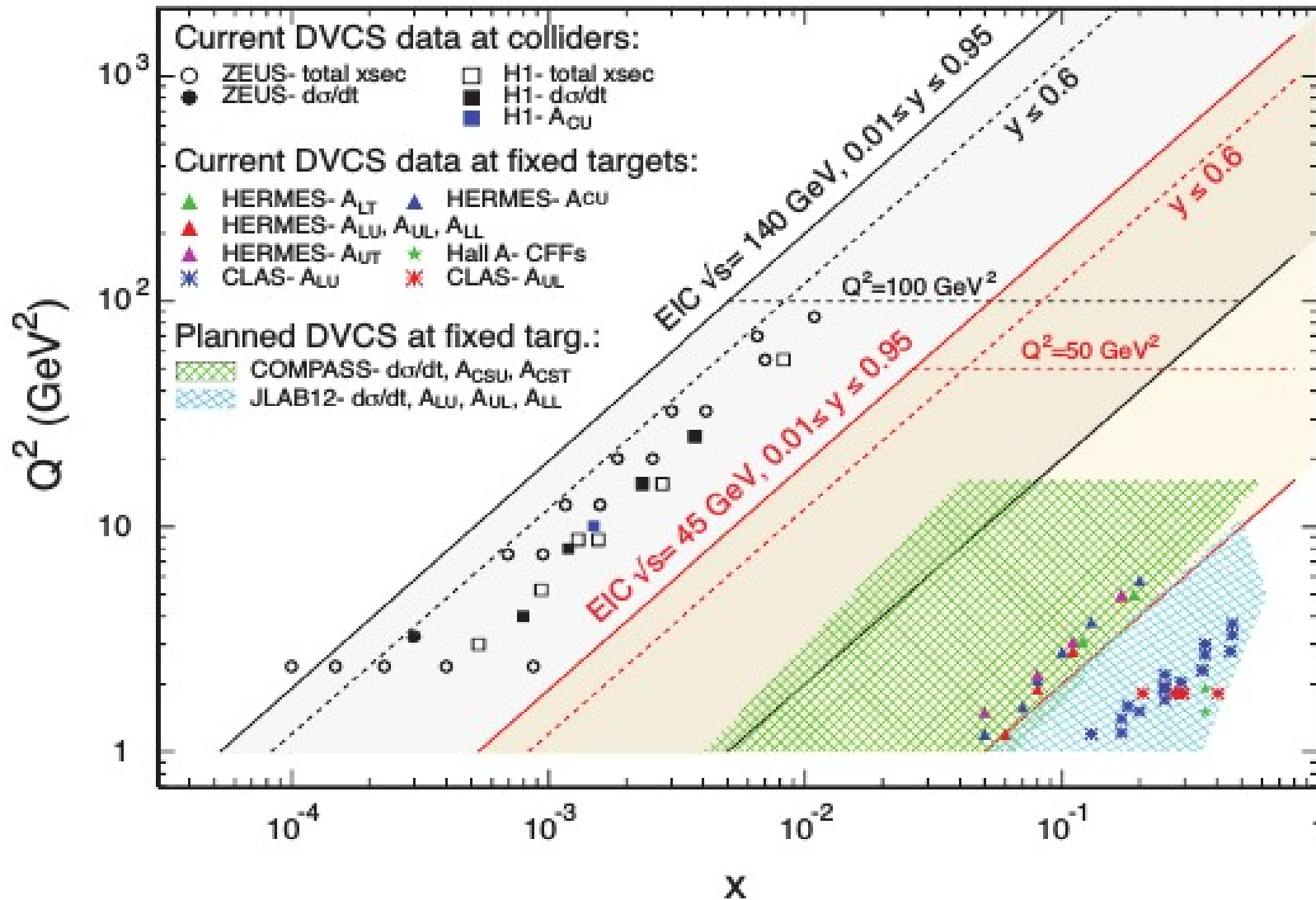
- High Intensity High Cooling
- Fixed Photon Beam
- Fixed NMR Sampling
- Manage Beam Heating
- Radiation Damage



Prospects for Better Experiment

- Higher Energy is Advantageous for TCS
 - BH is smaller
 - Invariant Mass of lepton pair is larger
- Fermilab Photon Beam
 - Primary Production Target
 - Bremsstrahlung
 - Purity/Monochromatic/Intensity/Tagged

Hi Resolution Imaging



Conclusion

- Get More from the Physics with PT observables
- Tensor Polarized Observables Largely Unexplored (Big Part of Spin Physics)
- Can isolate Twist-3 GPDs of the vector and axial vector sector with T/S-like combination
- Many more fun things to do with PT

Thank You

Take a look

Extraction of Generalized Parton Distribution Observables from Deeply Virtual Electron Proton Scattering Experiments

Brandon Kriesten,^{*} Simonetta Liuti,[†] Liliet Calero Diaz,[‡] Dustin Keller,[§] and Andrew Meyer[¶]

Department of Physics, University of Virginia, Charlottesville, VA 22904, USA.

Gary R. Goldstein^{**}

Department of Physics and Astronomy, Tufts University, Medford, MA 02155 USA.

J. Osvaldo Gonzalez-Hernandez^{††}

INFN, Torino

- i) Be General and Covariant*
- ii) Provide Kinematic Phase Separation*
- iii) Provide Clear Information Extraction*